DEPARTAMENTO DE CIÊNCIAS DA VIDA

FACULDADE DE CIÊNCIAS E TECNOLOGIA
UNIVERSIDADE DE COIMBRA

The effect of silver nanoparticles: a chronic *in vivo* study for the evaluation of hepatic mitochondrial toxicity

Dissertação apresentada à Universidade de Coimbra para cumprimento dos requisitos necessários à obtenção do grau de Mestre em Bioquímica, realizada sob a orientação científica do Doutor João Teodoro (Centro de Neurociências e Biologia Celular) e do Professor Doutor Carlos Manuel Marques Palmeira (Departamento de Ciências da Vida, Faculdade de Ciências e Tecnologia, Universidade de Coimbra)

RUI GONÇALO TEIXEIRA DA SILVA

2014

Agradecimentos

Gostaria de agradecer a todos aqueles que, directa ou indirectamente, contribuíram para que este trabalho se realizasse.

Em primeiro lugar, agradeço ao Professor Doutor Carlos Palmeira e à Professora Doutora Anabela Rolo por me terem recebido no seu laboratório e me terem dado a oportunidade de dar os meus primeiros passos enquanto investigador.

Ao Doutor João Teodoro, meu orientador, quero deixar um agradecimento muito especial. Agradeço-te sinceramente por todo o auxílio que me deste na realização deste trabalho. A tua disponibilidade, paciência e incentivo ajudaram muito a que este trabalho chegasse a bom porto. Agradeço-te também por todos os conselhos e ensinamentos que me transmitiste. Sem dúvida que te devo muito pelo meu desenvolvimento como cientista. Obrigado.

Um agradecimento muito especial para os meus colegas do MitoLab por toda a ajuda, conselhos, pela vossa amizade e pelos momentos de boa disposição partilhados Obrigado Ana, Filipe, João, Inês e Helena.

Aos meus colegas de Bioquímica, em particular ao Rúben, Tadeu, JP, Apóstolo e Zé Dias por todos os momentos inesquecíveis vividos ao longo destes 5 anos. À Pombo, Anita, Dani, Helena e Bruno pela vossa amizade e apoio.

Agradeço à minha família todo o apoio incondicional, em especial à minha Mãe. Agradeço-te do fundo do coração todo o esforço que fizeste para me manteres a estudar e por teres sempre apoiado as minhas decisões. Espero um dia te puder retribuir tudo aquilo que me proporcionaste.

À Catarina por todo o carinho, suporte e incentivo que me deram forças nos momentos menos bons.

Index

List of Figures and Tables

Chapter 4- Discussion and Conclusion

Abbreviations

ΔΨ- Mitochondrial membrane potential
Δ*p*- Proton motive force
ΔpH- pH gradient
ADP- Adenosine diphosphate
Ag^{+}- Silver
AgNPs- Silver nanoparticles
AIF- Apoptosis-inducing factor
ALT- Alanine aminotransferase
ANT- Adenine nucleotide translocase
AST- Aspartate aminotransferase
ATP- Adenosine triphosphate
Bax- Bcl-2–associated X protein
Bak- Bcl-2 homologous antagonist /killer
Bcl2 - B-cell lymphoma 2, apoptosis regulator protein
BSA- Bovine serum albumin
Ca^{2+}- Calcium ion
CK- Creatine kinase
COX- Cytochrome *c* oxidase
CsA- Cyclosporine A
Cyclo D- Cyclophilin D
DCF- 2′,7′-dichlorofluorescein
DNA- Deoxyribonucleic acid
EDTA- Ethylenediamine tetraacetic acid
EGTA- Ethylene glycol-bis(2-aminoethylether)-N,N,N’,N’-tetraacetic acid
ER- Endoplasmic reticulum
ETC- Electron transport chain
FCCP- Carbonyl cyanide 4-(trifluormethoxy) phenylhydrazone
$FADH_2$- Flavin adenine dinucleotide (reduced form)
GPx- Glutathione peroxidase
GSH- Glutathione
GST- Glutathione *S*-transferase
H^{+}- Proton
H_2DCF-DA- 2′,7′-Dichlorodihydrofluorescin diacetate
H_2O_2 - Hydrogen peroxide
HEPES- N-(2-hydroxyethyl)piperazine-N’-(2-ethanesulphonic acid)
HK- Hexokinase
IAPs- Inhibitor of Apoptosis Proteins
JNK- *c*-Jun N-terminal kinase
LDH- Lactate dehydrogenase
MAPK- Mitogen activated protein kinase

MOMP- Mitochondrial outer membrane permeabilisation
MPT- Mitochondrial permeability transition
mtDNA- Mitochondrial DNA
NAC- N-acetylcysteine
NADH- Nicotinamide adenine dinucleotide, reduced form
NPs- Nanoparticles
O- singlet oxygen molecules
O_2- molecular oxygen
$O_2^{\bullet-}$- Superoxide radical
$OH^{\bullet}$- Hydroxyl radical
OXPHOS- Oxidative phosphorylation
PBR- Peripheral benzodiazepine receptor
P_i- Inorganic phosphate
PMS- Phenazinemetosulphate
RaM- Rapid mode of calcium uptake
RES- Reticuloendothelial system
RCR- Respiratory control ratio
RFUs- Relative fluorescence units
ROS- Reactive oxygen species
rRNA- Ribosomal RNA
siRNA- Small interfering RNA
SDH- Succinate dehydrogenase
SMAC- Second mitochondria-derived activator of caspases
SOD- Superoxide dismutase
TBS- Tris-buffered saline
TCA cycle- Citric acid cycle, also known as Krebs cycle
TNF-α- Tumor necrosis factor
TMPD- Tetramethylphenylene-diamine
TPP^+- Tetraphenylphosphonium
tRNA- Transfer RNA
VDAC- Voltage dependent anion channel

Abstract

Manufactured nanomaterials have been of extreme importance due to the beneficial physicochemical properties they possess compared to bulk parental materials. However, the properties that make them so attractive are also the same that can cause harm both to humans and environment. Over the last years there has been a rapid development of the nanotechnology industry and the inevitable human exposure tends rapidly to expand, accompanied by potential for adverse health effects.

Among all used nanoparticles (NPs), silver nanoparticles (AgNPs) have the highest level of commercialization. Silver has been used for decades in medical healthcare due to its known antibacterial properties. One can also observe AgNPs in products used daily such as cosmetics, lotions, toothpastes, soaps, sunscreen, clothing and electronics. Over the last years, nanoparticles have been the subject of intense research for use in biomedicine, namely as biosensors, drug-delivery agents and imaging contrast agents, which take advantage of their unique optical properties.

Human exposure to AgNPs can occur through different ways: inhalation, ingestion, injection and dermal contact. As a major organ of detoxification, the liver is one of the most important targets after AgNPs exposure. The main toxicological concern is the fact that AgNPs preferentially accumulate in mitochondria. Since mitochondria have an essential bioenergetic function, impairment of mitochondria by nanoparticles may have drastic consequences on cellular function.

The mechanism by which AgNPs cause toxicity is still subject to uncertainty. However, oxidative stress has been related with the AgNPs toxicity. Therefore, antioxidant therapy might be a viable strategy for attenuating this toxicity.

In this work, we evaluated the toxicity of silver nanoparticles (10- and 75 nm) and their effects in rat liver mitochondrial bioenergetics. *In vivo* exposure to AgNPs was capable of increasing plasmatic aspartate aminotransferase (AST) and lactate dehydrogenase (LDH) activities, suggesting hepatocellular injury. Mitochondria isolated from animals treated with both AgNPs sizes showed a significant increase on reactive oxygen species (ROS) generation. Moreover, AgNPs caused impairment of rat liver mitochondrial function, mainly due to alterations of mitochondrial membrane permeability leading to an uncoupling effect on the oxidative phosphorylation system. AgNPs also compromised the electron transfer along the electron transport chain by

affecting the activity of complexes II and IV of the respiratory chain and interfered with the mitochondrial permeability transition (MPT) induction.

We found that most of the effects caused by AgNPs exposure were prevented by pretreatment with N-acetylcysteine (NAC). This antioxidant agent efficiently prevented the structural damage in the inner mitochondrial membrane as well as damage to mitochondrial electron transport chain complexes. Oxidative phosphorylation and calcium retention capacities of hepatic mitochondria were also improved by NAC treatment. The preventive effect of NAC efficiency was higher in 75 nm- than 10 nm-AgNPs, suggesting that smaller NPs have higher cytotoxicity than larger NPs.

In summary, our results indicate that the liver is a target of AgNPs exposure leading to alteration in hepatic mitochondria functions. Thus, the mitochondrial toxicity may have a central role in the toxicity resulting from exposure to silver nanoparticles. The efficiency of NAC administration against AgNPs toxicity suggests that ROS are involved in the mitochondrial toxicity caused by AgNPs treatment.

Keywords:

Mitochondria

Silver nanoparticles

Hepatic toxicity

N-acetylcysteine

Resumo

Os nanomateriais manufacturados têm sido de extrema importância devido às características físico-químicas benéficas que possuem comparados com os mesmos materiais de maiores dimensões. Contudo, as propriedades que os tornam tão atraentes são as mesmas que podem causar dano ao ser humano e ao meio ambiente. Ao longo dos últimos anos tem-se assistido a um rápido desenvolvimento da indústria de nanotecnologia, e a inevitável exposição humana tende a aumentar rapidamente, acompanhada por potenciais efeitos adversos para a saúde.

Das diversas nanoparticulas utilizadas (NPs), as nanoparticulas de prata (AgNPs) têm o maior grau de comercialização. A prata tem sido utilizada ao longo de décadas em cuidados de saúde devido as suas propriedades antibacterianas. Podemos também observar a presença de AgNPs em produtos utilizados no quotidiano tais como, cosméticos, loções, pasta dentífrica, sabonetes, protector solar, vestuário e electrodomésticos.

Ao longo dos últimos anos, as nanopartículas têm sido objecto de intensa pesquisa para aplicação em biomedicina, nomeadamente como biosensores, agentes de entrega de fármacos e agentes de contraste de imagem, tirando partido das suas propriedades ópticas únicas.

A exposição humana a AgNPs pode acorrer de várias formas: inalação, ingestão, injeção ou via transdérmica. Como principal órgão de desintoxicação, o fígado é um dos alvos mais importantes após a exposição a AgNPs. A principal preocupação toxicológica é o facto de as AgNPs se acumularem preferencialmente nas mitocôndrias. Uma vez que as mitocôndrias possuem uma função bioenergética essencial, danos nas mitocôndrias causados pelas nanoparticulas podem acarretar consequências drásticas na função celular.

O mecanismo através do qual as AgNPs causam toxicidade é ainda incerto. No entanto, o stress oxidativo tem sido associado à toxicidade provocada pelas AgNPs. Desta forma, a terapêutica antioxidante pode revelar-se uma estratégia viável para atenuar essa toxicidade.

Neste trabalho avaliámos a toxicidade de nanopartículas de prata (10 e 75 nm) e os seus efeitos na bioenergética mitocondrial do fígado de rato. Exposição i*n vivo* a AgNPs revelou-se capaz de aumentar as actividades plasmáticas da aspartato aminotransferase

(AST) e da lactato desidrogenase (LDH), sugerindo dano hepatocelular. Mitocôndrias isoladas de fígado de animais tratados com AgNPs de ambos os tamanhos demonstraram um aumento significativo na geração de espécies reactivas de oxigénio (ROS). Além disso, as AgNPs causaram danos na função mitocondrial principalmente devido a alterações na permeabilidade da membrana, provocando um efeito desacoplador no sistema de fosforilação oxidativa.

As AgNPs comprometem também a transferência de eletrões ao longo da cadeia transportadora devido ao facto de afetarem as atividades dos complexos II e IV da cadeia respiratória e interferirem também com a indução da transição de permeabilidade mitocondrial (MPT).

Demonstramos que a maioria dos efeitos causados pela exposição as AgNPs podem foram prevenidos pelo pré-tratamento com N-acetilcisteína (NAC). Este agente antioxidante impediu eficientemente a grande maioria dos efeitos das AgNPs nas mitocôndrias hepáticas. A fosforilação oxidativa e a capacidade de retenção de cálcio das mitocôndrias hepáticas foram também melhoradas através do tratamento com NAC. O efeito preventivo do NAC foi maior nas AgNPs de 75 nm do que nas de 10nm, sugerindo que NPs mais pequenas apresentam maior citotoxicidade quando comparadas com NPs de maiores dimensões.

Em suma, os nossos resultados demonstram que o fígado é um alvo da exposição a AgNPs conduzindo a alterações na função das mitocôndrias hepáticas. Desta forma, a toxicidade mitocondrial pode desempenhar um papel fulcral na toxicidade resultante da exposição a nanopartículas de prata. A eficácia da administração do NAC contra a toxicidade das AgNPs sugere que os ROS estão envolvidos na toxicidade mitocondrial provocada pela exposição às AgNPs.

Chapter I

General introduction

Over the last decades there has been a rapid development of the nanotechnology industry. It has promised great benefits both economic and scientific that will have application in areas as distinct as aerospace engineering, electronics, environmental remediation and medical healthcare. Manufactured nanomaterials have been of extreme importance to the industry due to the particular physicochemical features they possess compared to bulk parental materials. The most important of them comprise improved thermal and/or electrical conductivity, harder and stronger materials, improved catalytic activity and advanced optical properties (N. Singh et al., 2009). As we discover new uses for nanomaterials, the number of products containing them and their application will continue to grow exponentially. Thereby nanomaterials released from industrial activities and consumer products to the environment will increase and may accumulate in plants and animals. The bioaccumulation and propagation of nanomaterials through food chains is one of the biggest concerns in nanotoxicology (Bartłomiejczyk et al., 2013).

Nanomaterials range in size from 1 to 100 nm and they can take many different forms such as tubes, rods, wires or spheres. These nanomaterials can also have different dimensions. Thin films and engineered surfaces are examples of one-dimensional nanomaterials. On the other hand, there are nanomaterials in two dimensions for instance, carbon nanotubes, inorganic nanotubes, nanowires and biopolymers and nanomaterials in three dimensions such as nanoparticles, fullerenes (C_{60}), dendrimers and quatum dots (The Royal Society and The Royal Academy of Engineering 2004).

1.1. Silver Nanoparticles

Among all used nanoparticles (NPs), silver nanoparticles (AgNPs) have the highest level of commercialization (Figure 1.1) (Ahamed et al., 2010). AgNPs are often synthesized by a chemical reduction of a silver salt ($AgNO_3$) dissolved in water with a reducing compound such as sodium borohydride ($NaBH_4$), citrate, glucose, hydrazine and ascorbate (Marambio-Jones & Hoek, 2010; Tolaymat et al., 2010).

Silver has been used for decades in medical healthcare due to its known antibacterial properties (Carlson et al., 2008; Costa et al., 2010; Tolaymat et al., 2010). Thereby, AgNPs are widely used in medical devices such as wound dressings, medical catheters, contraceptive devices, bone prostheses and surgical instruments (Tolaymat et

al., 2010). One can also observe AgNPs in products used daily, for instance cosmetics, lotions, creams, toothpastes, soaps, sunscreen, clothing and electronics (Teodoro et al., 2011; Tolaymat et al., 2010).

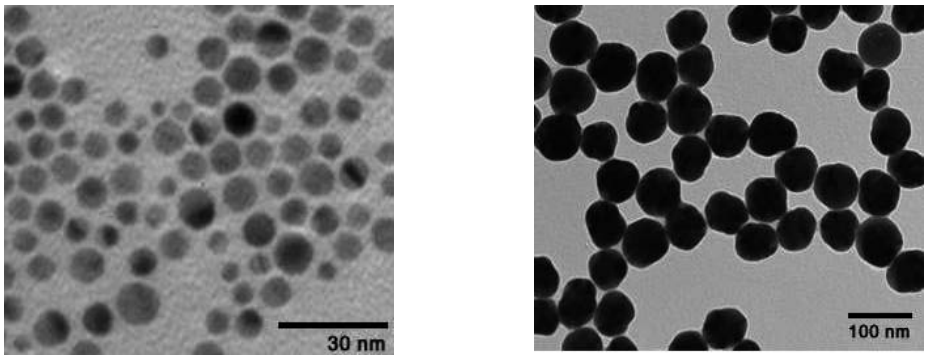

Figure 1.1- Transmission electron microscopy (TEM) image of silver nanoparticles with diameters of 10 nm and 75 nm, respectively.

The examples shown so far are related with unintentional exposure to NPs. However, there are some cases where exposure is made on purpose such as applications of NPs as biosensors, drug-delivery agents and imaging contrast agents (R. Zhang et al., 2012) as well as treatments of diseases that require constant drug concentration in the blood or targeting of specific cells (Ahamed et al., 2008). For instance, Elechiguerra and colleagues have shown that AgNPs undergo size-dependent interactions with the HIV-1 virus and inhibit its binding to the host cell *in vitro* (Elechiguerra et al., 2005).

As mentioned above, NPs have physicochemical properties that make them so useful and provide them advantages upon the bulk materials. The most important ones are the size, shape, crystallinity, surface charge and coating, elemental composition and solubility (Carlson et al., 2008). Nevertheless, the properties that make NPs attractive are also the same properties that can cause danger both to humans and environment (Carlson et al., 2008; Teodoro et al., 2011). Although some studies have reported these dangers, there is a serious lack of information about the role of NPs in biological systems. The studies made so far are scarce and sometimes conflicting, thus it is essential understand NPs toxicity, distribution, bioaccumulation as well as its excretion.

There are several factors that can influence stability and bioavailability of NPs such as particle size, shape, capping agents, pH, ionic strength, specific ions and ligands

(Marambio-Jones & Hoek, 2010). For instance, high salt levels and pH values close to the isoelectric point will enhance agglomeration, resulting in a larger hydrodynamic size (Jiang et al., 2008).

Once inside the cell, NPs can get metabolized and potential physicochemical changes can occur (Teodoro et al., 2011), especially hydrodynamic size and surface charge (Jiang et al., 2008) causing unpredictable behavior. Thus it is essential the characterization of these nanoparticles in solution.

1.1.1. Size

The nanometric size is one of the main features that provide NPs unique properties when compared with larger materials of the same composition. Their small size allows them to easily cross biological barriers and once inside the cell NPs can pass through membranes into critical organelles such as mitochondria and interact with biomolecules, which can be harmful to normal cellular functioning (Carlson et al., 2008; N. Singh et al., 2009). However, this ability to easily cross biological barriers could be advantageous when NPs are used on development of new nanomedicines and nanodevices for clinical healthcare.

All NPs, regardless of their chemical composition, have surface area:volume ratios that are extremely high (Table I). As the size decreases, the number of particles per unit of mass increases as well as its surface area. This larger surface area:volume ratios enhances the catalytic activity of the material and thus increases its reactivity with other molecules (N. Singh et al., 2009). Hence, it is suggested that size is one of the main characteristics responsible for cytotoxicity of AgNPs. Several studies have reported that smaller AgNPs induced more cytotoxicity than larger AgNPs (Ahamed et al., 2008; Carlson et al., 2008; Monteiller et al., 2007)

Smaller AgNPs can pass through cell membranes more efficiently than larger AgNPs and due to their smaller size they have a larger surface area available for interaction with cellular organelles. Moreover, the higher surface area allows smaller AgNPs to enhance release of Ag^+ ions from their surface (Kim & Ryu, 2013). AgNPs release Ag^+ in the presence of water (Kim & Ryu, 2013; Lee et al., 2013; Tiwari et al., 2011) probably due to surface oxidation and this release of Ag^+ ions might lead to an amplification of AgNPs toxicity (R. Zhang et al., 2012).

Nanosphere Diameter (nm)	Surface area (nm^2)	Volume (nm^3)	Ratio Surface Area:Volume
10	314	523	0.60
20	1260	4190	0.30
30	2830	14100	0.20
40	5030	33500	0.15
50	7850	65500	0.12
60	11300	113000	0.10
70	15400	180000	0.09
80	20100	268000	0.08
90	25400	382000	0.07
100	31400	523600	0.06

Table I - Diameter, Surface area and Volume of nanosphere (Source: www.nanocomposic.com)

1.1.2. Shape

With regards to shape, there are some reports showing different rates of uptake depending on the type of nanoparticles shape. For instance, spherical nanoparticles have shown higher uptake than nanorods (N. Singh et al., 2009).

Many nanomaterials have an inherent property, their hydrophobicity and as result a likelihood to agglomerate/aggregate mainly under physiological conditions (Kim & Ryu, 2013; N. Singh et al., 2009). Therefore when NPs are in a biological system, it is likely that it will be in the form of aggregates rather than individual units. Thus, in such conditions NPs might no-longer be in nano size range. Thus, their effects upon biological systems may be considerably lower probably due to reduced cellular uptake or an inability to cross biological barriers (N. Singh et al., 2009). This problem of aggregation can be overcome modifying the surface of nanomaterials with capping agents. A capping agent is used to promote stability of NPs, resulting in a surface

polarity that prevents aggregation of nanoparticles due to electrostatic repulsion (El Badawy et al., 2010). Sodium citrate is the most common capping agent used (Tolaymat et al., 2010). Citrate-capped AgNPs have negative surface charge due to the carboxylic moiety of the citrate and this negative charge increases the repulsion between NPs and prevents aggregation (Figure 1.2) (Park & Lee, 2013). Thus the cellular uptake increases, overloading the cellular systems with nanoparticles. Murdock et al., (2008) reported uncoated particles tend to agglomerate while coated are far more dispersed. Ahamed and colleagues showed differences between coated and uncoated NPs, demonstrating that coated AgNPs cause more severe problems than uncoated AgNPs (Ahamed et al., 2008).

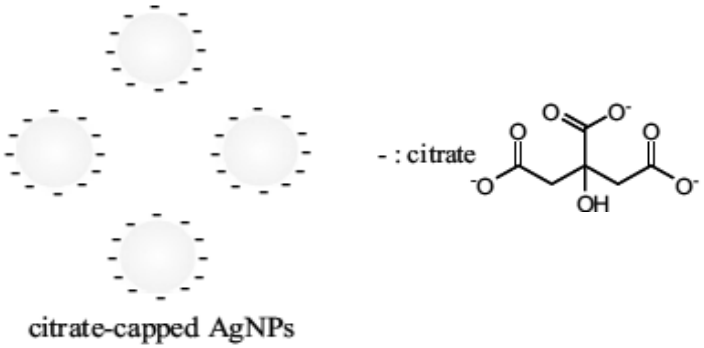

Figure 1.2- Schematic representation of citrate-capped AgNPs. Citrate has negative charge due to the carboxylic moiety giving to citrate-capped AgNPs negative surface charge. This negative surface charge increases the repulsion between NPs preventing aggregation (adapted from Zheng, Yu, Xu, & Chen, 2014).

1.1.3. Uptake

The uptake of NPs by cells depends on the size and shape of the particles, the surface charge, and the surface functionalization of the particles. Smaller NPs are internalized more efficiently compared to larger NPs.

Surface charge influences cellular uptake of nanomaterials because once the plasma membrane is negatively charged, nanomaterials with cationic surface charges (positively charged) may interact more efficiently with plasma membrane than those that are anionic (negatively charged) (N. Singh et al., 2009). Regarding to surface of

NPs, the surface chemistry can be altered by attachment of biomolecules for cell targeting or drug delivery.

In mammalian cells, NPs undergo uptake by mechanisms as phagocytosis, macropinocytosis, caveolae-dependent endocytosis, nonclathrin-, non-caveolae-mediated endocytosis, clathrin-dependent endocytosis, phagocytosis, and diffusion (Figure 1.3) (Asharani et al., 2009; Unfried et al., 2007). Regarding to AgNPs, clathrin-dependent endocytosis and macropinocytosis have been shown to be the primary uptake mechanism on *in vitro* studies (Asharani et al., 2009; Greulich et al., 2011). Using animal studies, Lee et al., (2013) shown that AgNPs were localized mainly in endosomes and lysosomes of hepatocytes. Therefore, these findings provide evidence regarding to previous *in vitro* reports describing the uptake of AgNPs occur mainly through endocytosis.

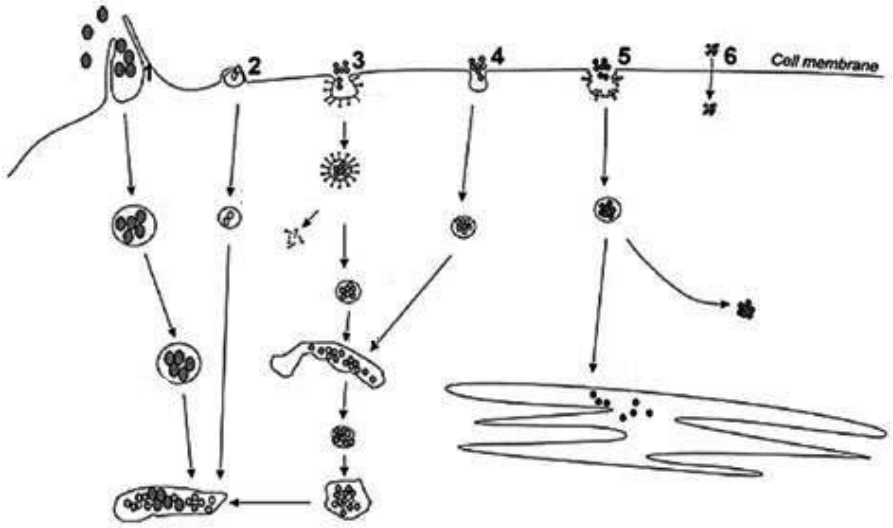

Figure 1.3 - Possible pathways of cellular uptake of nanoparticles in mammalian cells. 1-phagocytosis; 2-macropinocytosis; 3-clathrin-dependent endocytosis; 4- nonclathrin-, non-caveolae-mediated endocytosis; 5- caveolae- dependent endocytosis; 6-diffusion. (Unfried et al., 2007)

1.1.4. Human exposure

AgNPs are the focus of this report. Their widespread use and commercialization have raised concerns about human and environmental exposure. In humans, argyria, a

disease caused by exposure to high levels of silver, produces a benign bluish-gray discoloration of the skin and other organs (Carlson et al., 2008).

Human exposure to AgNPs can occur through different ways: inhalation, ingestion, injection and dermal contact (Ahamed et al., 2010; Lee et al., 2013). Once inside the body, AgNPs rapidly enter circulation and may migrate to liver, kidney, spleen, lungs and brain, inducing toxicity (Figure 1.4) (Aillon et al., 2009; Greulich et al., 2011; Singh & Ramarao, 2012). Liver and spleen have been identified as the main target organs for nanomaterials after injection. Liver, as a major organ of detoxification, might retain nanoparticles due to the presence of specific subpopulations of mononuclear phagocytic cells which are part of the reticulo-endothelial system (RES) (Dziendzikowska et al., 2012).

Important elements of RES are the Kupffer cells that play a crucial role in the removal of nanoparticles from the organism (Sadauskas et al., 2007). Lee and colleagues observed that AgNPs deposited in Kupffer cells after treatment (Lee et al., 2013). Excessive accumulation of AgNPs in the liver can lead to certain adverse effects such as pathological changes in liver morphology, generation of reactive oxygen species (ROS), DNA damage and changes in liver enzyme activities (Tiwari et al., 2011).

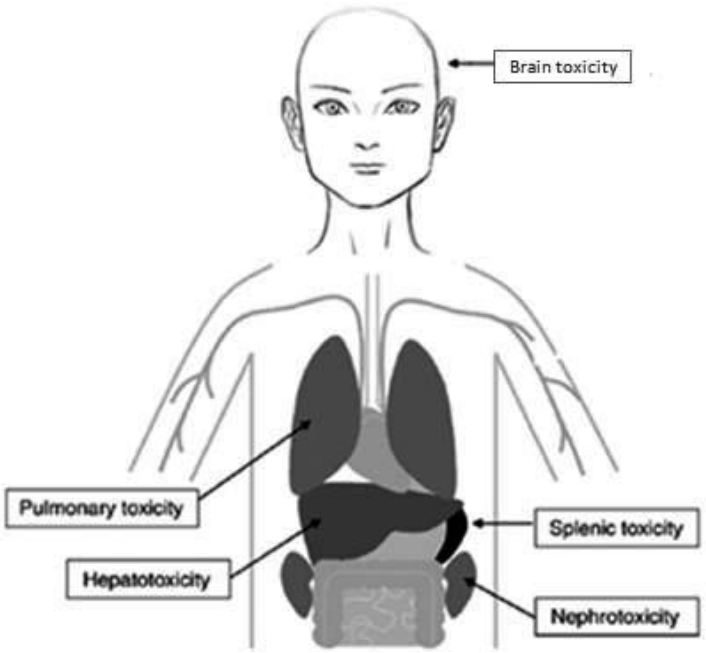

Figure 1.4- Main forms of *in vivo* silver nanoparticles. Once inside the body, silver nanoparticles may migrate to liver, kidney, spleen, lungs and brain, inducing toxicity (adapted from Aillon et al., 2009).

1.1.5. Mechanisms of toxicity

The mechanism by which AgNPs cause toxicity is still subject to uncertainty. Some researchers suggested that AgNPs might act as a "Trojan horse", crossing biological barriers and then releasing Ag^+ ions that are the main cause for cell damage. Alternatively, some studies suggested that both AgNPs as well as Ag^+ ions are responsible for AgNPs toxicity (Ahamed et al., 2010). Thus, it is important understand whether Ag^+ ions are the only cause of the toxicity of AgNPs or if NPs have also toxicity distinct from that of ionic silver.

1.1.6. ROS production

Silver, a soft metal, displays a strong affinity for thiol (–SH) groups present in biomolecules found throughout the body, as for example protective antioxidant agents. Thus, it is possible that AgNPs might cause an imbalance on human health due to an increase of oxidative stress. Metals can act as catalysts and generate ROS in the presence of dissolved oxygen. Therefore, this could be a mechanism by which silver nanoparticles increase oxidative stress. Both *in vitro* and *in vivo* studies have shown that AgNPs lead to ROS production (Arora et al., 2008; Carlson et al., 2008; Ghosh et al., 2012; Tiwari et al., 2011) and thereby these studies are in agreement with the previous hypothesis that oxidative stress is one of the main mechanisms which NPs exert their toxicity (Monteiller et al., 2007). Arora et al., (2008) found that exposure to AgNPs caused depletion of glutathione (GSH) and increased lipid peroxidation, clear signals of oxidative stress. Moreover, Hussain et al., (2005) showed a significant increase in ROS on BRL 3A liver cells following AgNPs treatment.

ROS are a general term used to describe molecules and free radicals derived from molecular oxygen: singlet oxygen molecules (O), superoxide anions ($O_2^{\bullet-}$), hydrogen peroxide (H_2O_2) and the most potent oxidizing agents, hydroxyl radicals ($OH^{\bullet}$). Therefore, ROS are produced as byproducts of cellular oxygen metabolism. The majority of oxygen consumption in the cell occurs through oxidative phosphorylation, and as such mitochondria are the primary source of ROS in the cell.

Under environmental stress, the cell ROS generation increases, which in turn leads to an imbalance between ROS generation and their elimination by antioxidant agents.

This imbalance of the redox equilibrium is called oxidative stress and may cause transient or even permanent damage to proteins, lipids and nucleic acids, and these cumulative alterations can eventually kill the cell by apoptosis or necrosis.

Eukaryotic organisms have developed a variety of enzymatic and nonenzymatic systems to eliminate ROS and try to repair their effects. The most important ones are superoxide dismutase (SOD), catalase, glutathione peroxidase (GPx), glutathione S-transferase (GST), peroxiredoxins, glutathione (GSH) and vitamins. Among all of these antioxidant scavengers, GSH plays a major role in cellular protection against oxidative stress due to its ability to bind and reduce ROS (Kim & Ryu, 2013).

ROS play important roles in normal biochemical functions in the cells such as cell signaling and abnormality in ROS metabolism results in pathological processes. For example, it is known that excessive production of ROS can induce apoptosis (Martindale & Holbrook, 2002). Several studies have shown that ROS production leads to apoptotic processes followed by AgNPs treatment (Ahamed et al., 2010; Carlson et al., 2008).

N-acetylcysteine (NAC) is a precursor of the synthesis of GSH and thus is an important antioxidativo compound. *In vitro* studies found that pretreatment with NAC prevented AgNPs toxicity in human liver cells and HepG2 (Jing et al., 2011; Kim et al., 2009), suggesting that the main mechanism of AgNPs toxicity is associated with oxidative damage-dependent pathways.

1.1.7. Apoptosis

Apoptosis is a form of programmed cell death, where occurs a shutdown of metabolism and digestion of cell contents. Apoptosis takes place when the damage in cells, especially that affecting DNA, is beyond repair and cells activate enzymes that degrade their own DNA (Kim & Ryu, 2013). The machinery of apoptosis is composed of caspases, caspase activators, B-cell lymphoma 2 (Bcl-2) family of proteins and inhibitor of apoptosis proteins (IAPs) (Bernardi et al., 1999). Caspases are cysteine proteases that play a key role in the apoptotic cascade and the proteolytic digestion of the cell. Caspases exist as inactive precursor procaspases and are activated by controlled proteolytic cleavage. The Bcl-2 family of proteins is a group of mitochondrial proteins that participate in the modulation of the apoptotic phenomenon. This family includes

both pro- and anti-apoptotic members that largely localize to the outer mitochondrial membrane. The pro-apoptotic BH3-only family members (Bid, Bad, Bim, Noxa and Puma) activate the pro-apoptotic proteins Bax and Bak while anti-apoptotic (Bcl-2, Bcl-xl, Blc-w and Mcl-1) members tend to inhibit them. The balance between pro-apoptotic and anti-apoptotic protein levels is crucial for the cell's fate (Bernardi et al., 1999).

1.1.8. Inflammation

Besides activation of apoptosis, oxidative stress may also activate specific signaling pathways such as mitogen activated protein kinase (MAPK) and release of pro-inflammatory cytokines (Bartłomiejczyk et al., 2013). The activation of these signaling cascades causes inflammation which in turn leads to further ROS generation from inflammatory cells, resulting in a vicious cycle (N. Singh et al., 2009). It was shown that AgNPs increase the secretion of inflammatory cytokines in macrophages cell lines (Carlson et al., 2008). The c-Jun-N-terminal kinase (JNK) is a member of the MAPK family and plays a proapoptotic function in response to oxidative stress leading to apoptosis (Hsin et al., 2008).

Some studies reported that DNA damage could occur after AgNPs treatment. Arora et al., (2009) demonstrated that AgNPs could cause DNA damage in fibroblast and liver cells and Ahamed et al., (2008) also found DNA damage after AgNPs exposure.

The increase of oxidative stress and inflammatory responses may cause DNA damage (N. Singh et al., 2009), leading to the activation of p53. The p53 protein is a tumor suppressor gene and when DNA is damaged, p53 is able to activate cell cycle checkpoints and the transcription of genes responsible for DNA repair, in an attempt to avoid the propagation of damage. However, if the damage is too extensive to be repaired, p53 induces activation of proapoptotic factors such as Bcl 2-associated X protein (BAX), triggering apoptosis to eliminate the individual cell for the benefit of the organ. Thus the activation of p53 can be a good marker for assessing NPs genotoxicity. *In vitro* studies shown activation of p53 after AgNPs administration (Ahamed et al., 2008; Hsin et al., 2008).

1.2 Mitochondria

Mitochondria are the only organelles that contain extra-nuclear DNA and have a replication system independent from nuclear DNA replication. Human mitochondrial DNA (mtDNA) is a 16 600 base pairs circular, double-stranded molecule, encoding 11 mRNAs that give rise to 13 subunits of the oxidative phosphorylation system, 22 transfer RNAs (tRNAs) and two ribosomal RNAs (rRNAs). However, most of the mitochondrial proteins are nuclear-encoded and imported into the mitochondria (Lagouge & Larsson, 2013).

Mutations in genes encoding mitochondrial components cause mitochondrial dysfunction. This mitochondrial dysfunction has been related with the development of metabolic disorders like insulin resistance and diabetes, aging process as well as cardiovascular and neurodegenerative diseases (Rolo & Palmeira, 2006; Santos et al., 2013; Shoubridge, 2001).

Mitochondria are the powerhouses of the cells since they produce more 95% of cell's total energy requirement (Costa et al., 2010). Thus mitochondria are essential organelles for cell survival and growth. The number of mitochondria present in each cell depends upon their metabolic requirements and may range from hundreds to thousands. Unlike what was thought to a few years ago, mitochondria are dynamic organelles since they continuously change their shape and numbers through frequent fusion, fission and movement throughout the cell (McBride et al., 2006), processes that are intimately linked to the cell's energetic needs.

The most well known function of mitochondria involves the production of chemical energy through the electron transport chain (ETC). However, besides energy production, mitochondria assume other functions such as heme synthesis, β-oxidation of free fatty acids, metabolism of certain amino acids, formation and export of Fe/S clusters, iron metabolism, and play also a crucial role in calcium homeostasis and cell death (Michel et al., 2012).

1.2.1 Mitochondrial Structure

A double phospholipid membrane limits the structure of the mitochondria, the outer and inner membrane (Figure 1.5). The outer membrane separates the mitochondrion

from the cytosol and encompasses the whole organelle. It main protein is the voltage-dependent anion channel (VDAC), responsible for the passage of low molecular-weight molecules between the cytoplasm and the intermembrane space. The intermembrane space is an important compartment on mitochondria, since it acts as a reservoir of protons (H^+) establishing a H^+ electrochemical gradient (with electric and pH components) across inner membrane that is essential for the production of ATP via ATP synthase. Most of this gradient is in form of electrical potential difference.

The inner membrane forms invaginations towards the internal matrix, designated by cristae, increasing the surface area of this membrane. Unlike the outer membrane, the inner membrane is largely impermeable to most ions and polar molecules, including protons. For that reason, solutes can only cross it through highly regulated and selective channels. The inner membrane houses the respiratory enzymes of the ETC and many mitochondrial carriers. Within the matrix, different metabolic pathways take place including tricarboxylic acid (TCA) or Krebs cycle that generate reducing equivalents such as nicotinamide adenine dinucleotide (NADH) and flavin adenine dinucleotide ($FADH_2$) which then donate electrons to the ECT and β-oxidation breaks down fatty acid molecules to generate Acetyl-Coenzyme A (Acetyl-CoA) which enters the Krebs cycle.

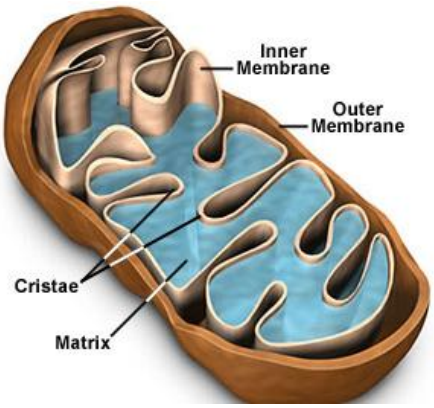

Figure 1.5- Mitochondrial morphology. Mitochondria are a double membrane-system: the outer membrane separates the mitochondrion from the cytosol and defines the outer perimeter and the inner membrane, that is invaginated, forms the cristae and defines the matrix of the organelle.

1.2.2 Electron Transport Chain

Four enzymatic protein complexes, complexes I-IV, comprise the ETC. Electrons deriving from oxidation of substrates pass through the redox carriers until finally reduce molecular oxygen to form water. This electronic transport allows for the vectorial ejection of protons across the inner mitochondrial membrane, from the matrix towards the intermembrane space. This creates an electrochemical protonic gradient which can be used by Complex V, or ATP synthase, to drive the phosphorylation of adenosine diphosphate (ADP). These processes involve the coupling of both redox and phosphorylation reactions in the inner membrane of mitochondria, resulting in an effective ATP synthesis. To this it is called oxidative phosphorylation (OXPHOS).

NADH-ubiquinones oxidoreductase (Complex I) accepts electrons from nutrients via reduced form of NADH, which then are transported to oxidized ubiquinone (a mobile intramembrane protein), originating its reduced form, ubiquinol. Ubiquinone can also accept electrons from the reduced form of $FADH_2$, originated from succinate, at succinate-ubiquinone oxidoreductase (Complex II). Ubiquinol, a highly mobile protein, will then transfer electrons to ubiquinone-cytochrome *c* oxidoreductase (Complex III) and from here to cytochrome *c*, another mobile protein from the intermembrane space, which will reduce cytochrome *c* oxidase (Complex IV). Here, the electrons are transferred to the final electron acceptor, molecular oxygen (O_2), generating H_2O. It is important to notice that this electronic transport is only possible due to the increasingly energetic favorable electronic jumps between proteic complexes. The released energy from these electronic jumps is used by Complexes I, III and IV to drive the protonic ejection against its concentration gradient.

As mentioned, the consequent movement of the H^+ creates an electrochemical gradient due to the low protonic conductance of the inner mitochondrial membrane. This electrochemical gradient consists of a pH gradient (ΔpH) and an electrical gradient that are used to drive the synthesis of ATP from ADP as the protons re-flow through the ATP synthase proton channel (complex V) (Figure 1.6). After ATP synthesis the adenine nucleotide translocase (ANT) allows the exchange of ATP from mitochondrial matrix with ADP from cytosol.

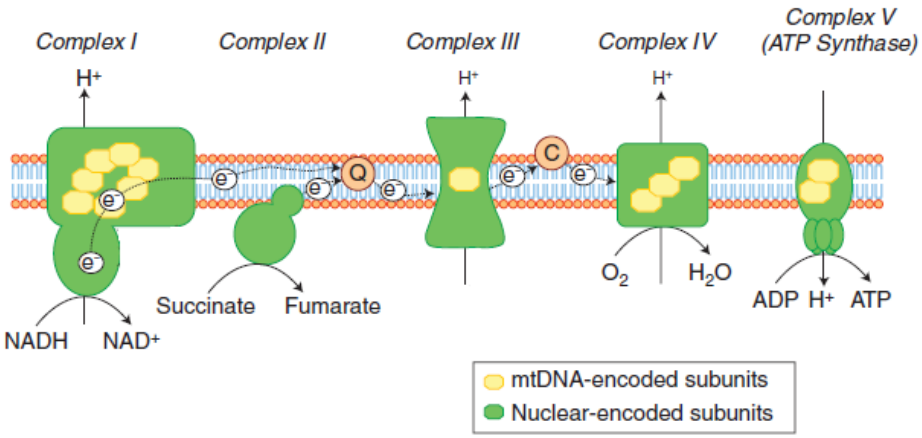

Figure 1.6- Schematic representation of electron transport chain (ETC). ETC is composed of approximately 100 proteins, 13 of which are encoded by the mtDNA. It consists of five protein complexes; complex I and complex II receive electrons (e^-) from intermediary metabolism, which are then transferred to coenzyme Q and subsequently delivered to complex III. Cytochrome *c* then transfers the e^- to complex IV, which constitutes the final step in the ETC in which molecular oxygen is reduced to water. The electron transport is coupled to proton (H^+) pumping across the inner membrane by complexes I, III and IV. The resulting proton gradient drives ATP synthesis through complex V (ATP synthase). C, cytochrome c; Q, coenzyme Q. (Image based on Perier & Vila, (2012))

OXPHOS is known as the prime location for ROS generation and thus, mitochondria are the first targets of oxidative damage. The generation of mitochondrial ROS is a normal consequence of OXPHOS because along the ETC electrons may escape and react with O_2 generating free radicals.

Complexes I and III are considered to be the main sites for ROS production in mitochondria (Rigoulet et al., 2011). Superoxide anion ($O_2^{\bullet -}$) is the primary ROS produced in mitochondria as a result of single electron transfer to oxygen in the respiratory chain. This species can directly attack biological molecules or be dealt with by native mitochondrial antioxidant defenses. $O_2^{\bullet -}$ can thus be reduced to hydrogen peroxide (H_2O_2) and this to molecular water and oxygen, by the combined actions of the antioxidant enzymes Superoxide dismutase and Glutathione peroxidase, respectively.

Under normal conditions, cells are able to deal with high levels of ROS through a variety of defense mechanisms. However, when ROS production overcomes the antioxidant defenses of the cell, this may cause transient or permanent damage to biological molecules. This cumulative damage can ultimately destroy the cell by

apoptosis or even necrosis. Within mitochondria, lipids, proteins, OXPHOS enzymes and mtDNA are particular vulnerable to free radicals (Pieczenik & Neustadt, 2007).

1.2.3 Mitochondrial permeability transition

Calcium (Ca^{2+}) is a potent and ubiquitous second messenger, capable of regulating dozens of biological processes, including proliferation, gene transcription, post-translational modification of proteins and aerobic metabolism (Rasola & Bernardi, 2011). Researchers have a great interest in mitochondrial Ca^{2+} transport because of the central role of mitochondria and intramitochondrial Ca^{2+} in programmed cell death. Once inside the cell, Ca^{2+} may be sequestered by intracellular organelles such as mitochondria and endoplasmic reticulum (ER). The physiological increase in mitochondrial Ca^{2+} has been observed to activate dehydrogenases coupled to the Krebs cycle as well as ATP synthase (Territo et al., 2000). This enhancement of enzymatic activity stimulates Krebs cycle and OXPHOS, and thus ATP synthesis.

Calcium enters the matrix of mitochondria through two modes of inward transport, Ca^{2+} uniporter and the rapid mode or RaM (Gunter et al., 2000). On the other hand, calcium efflux from mitochondria takes place mainly through mitochondrial sodium/calcium exchanger but the high conductance ion channels like mitochondrial permeability transition (MPT) pore is another important mechanism for Ca^{2+} release. The ability of mitochondria to accumulate Ca^{2+} is large but not infinite and when the limit is exceed there is a dramatic collapse of mitochondrial membrane potential which causes cessation of oxidative phosphorylation and ROS production; matrix swelling and cristae unfolding and rupture of the outer membrane with release of the accumulated Ca^{2+} and of apoptogenic proteins (Rasola & Bernardi, 2011)

The structure of the MPT pore is still a matter of intense debate, and its existence is not still completely demonstrated. What it is undoubtedly present is the phenomenon, the mitochondrial permeability transition. As the current model proposes, MPT pore is a multimeric protein channel complex formed by ANT, VDAC, peripheral benzodiazepine receptor (PBR), mitochondrial phosphate carrier, hexokinase (HK), creatine kinase (CK) and cyclophilin D (Cyclo D) (Figure 1.7) (Kroemer et al., 2007). Its opening increases membrane permeability to all solutes with molecular weight up to 1.5 kDa, under certain conditions such as Ca^{2+} overloading, presence of inorganic

phosphate (P_i) and other factors including oxidative stress (Rasola & Bernardi, 2011). This channel is voltage- and Ca^{2+}-dependent and cyclosporine A (CsA)-sensitive (Almofti et al., 2003).

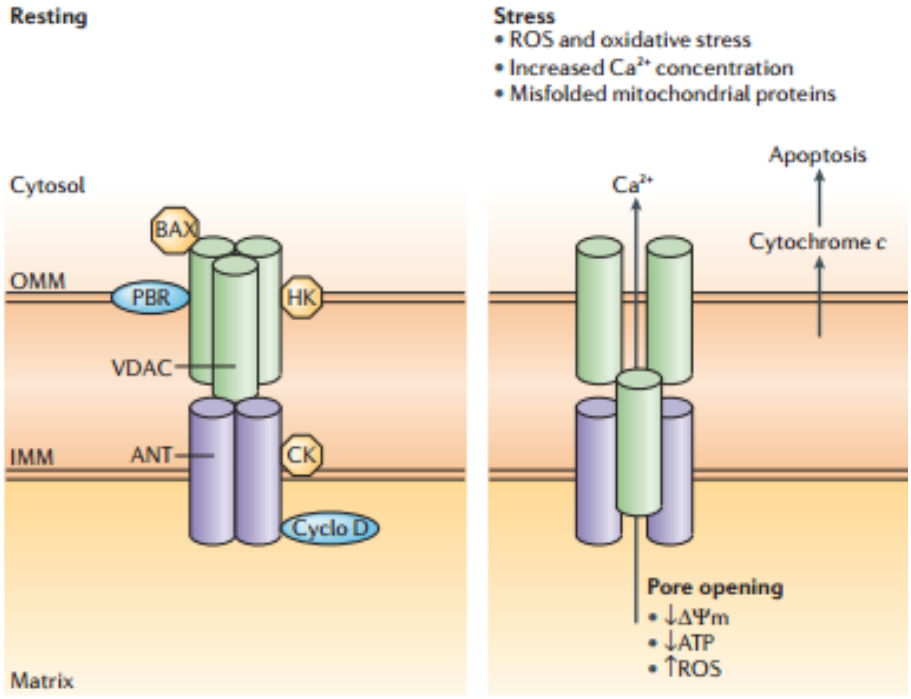

Figure 1.7- Induction of the mitochondrial permeability transition (MPT). The mitochondrial permeability transition (MPT) pore is a multimeric protein channel complex, between the inner and outer membranes, formed by the voltage-dependent anion channel (VDAC) on the outer mitochondrial membrane (OMM), the adenine nucleotide translocator (ANT) on the inner mitochondrial menbrane (IMM), and cyclophilin D (Cyclo D) in the matrix. Other proteins, such as the peripheral benzodiazepine receptor (PBR), hexokinase (HK) and creatine kinase (CK) are probably also involved in this phenomenon. Pathophysiological conditions, such as elevated Ca^{2+} concentrations, oxidative stress, ATP depletion and mitochondrial depolarization are known inducers of MPT, with consequent increase in the permeability of the IMM. The opening of the MPT pore ultimately results in mitochondrial swelling, mitochondrial Ca^{2+} efflux and the release of apoptogenic proteins, such as cytochrome *c* and procaspases, from the intermembrane space. ΔΨm, mitochondrial membrane potential; BAX, BCL2-associated X protein; ROS, reactive oxygen species (from Abou-Sleiman et al., (2006)).

The solute input to equilibrate ionic gradients of species with molecular mass lower than about 1.5 kDa leads to an increase in mitochondrial matrix volume due to water entry inside de mitochondria. This increase results in mitochondrial swelling associated with membrane depolarization and uncoupling of the mitochondria, calcium release, unfolding of the inner membrane cristae and rupture of the outer membrane (Bernardi et al., 1999). The breaches in the outer membrane allows the release of cytochrome c and other apoptogenic proteins stored in the intermembrane space, which in turn can activate effector caspases and apoptotic dismantling of the cell.

The general mitochondrial abnormalities linked with the phenomenon include mitochondrial electron transport chain impairment, anomaly in calcium homeostasis and alterations in mitochondrial morphology and dynamics. Their dysfunction can lead to a decline in energy production, generation of reactive oxygen species and induction of apoptosis.

1.2.4 Cell death

Necrosis and apoptosis are two different forms of cellular death. Whereas apoptosis requires a minimal amount of intracellular ATP, necrosis is generally accompanied by its total depletion (Kroemer et al., 2007). So, at least in part, the abundance of intracellular energy stores seems to be important to decide the form of cellular death.

Necrosis is characterized by a gain in cell volume that leads to rupture of the plasma membrane and the unorganized dismantling of swollen organelles, while apoptosis is characterized by organized systematic steps leading to the dismantling of the entire cell with minimal leakage of cell constituents (Kroemer et al., 2007).

Apoptosis is a crucial process of animal life that eliminates unwanted cells and is vital for embryonic development, homeostasis and immune defence (Ow et al., 2008). Apoptosis can occur mainly through two different pathways: the extrinsic and intrinsic pathway (Figure 1.8). The first one is mediated by death receptors (DR) located on the cell surface, induced by DR ligands (i.e., tumour necrosis factor (TNF-α), FasL), which originate death signals from the extracellular media to the inside of the cell. The intrinsic (or mitochondrial) pathway occurs in response to signals originated from inside the cell (Soane et al., 2007) such as DNA damage, metabolic stress or the presence of unfolded proteins.

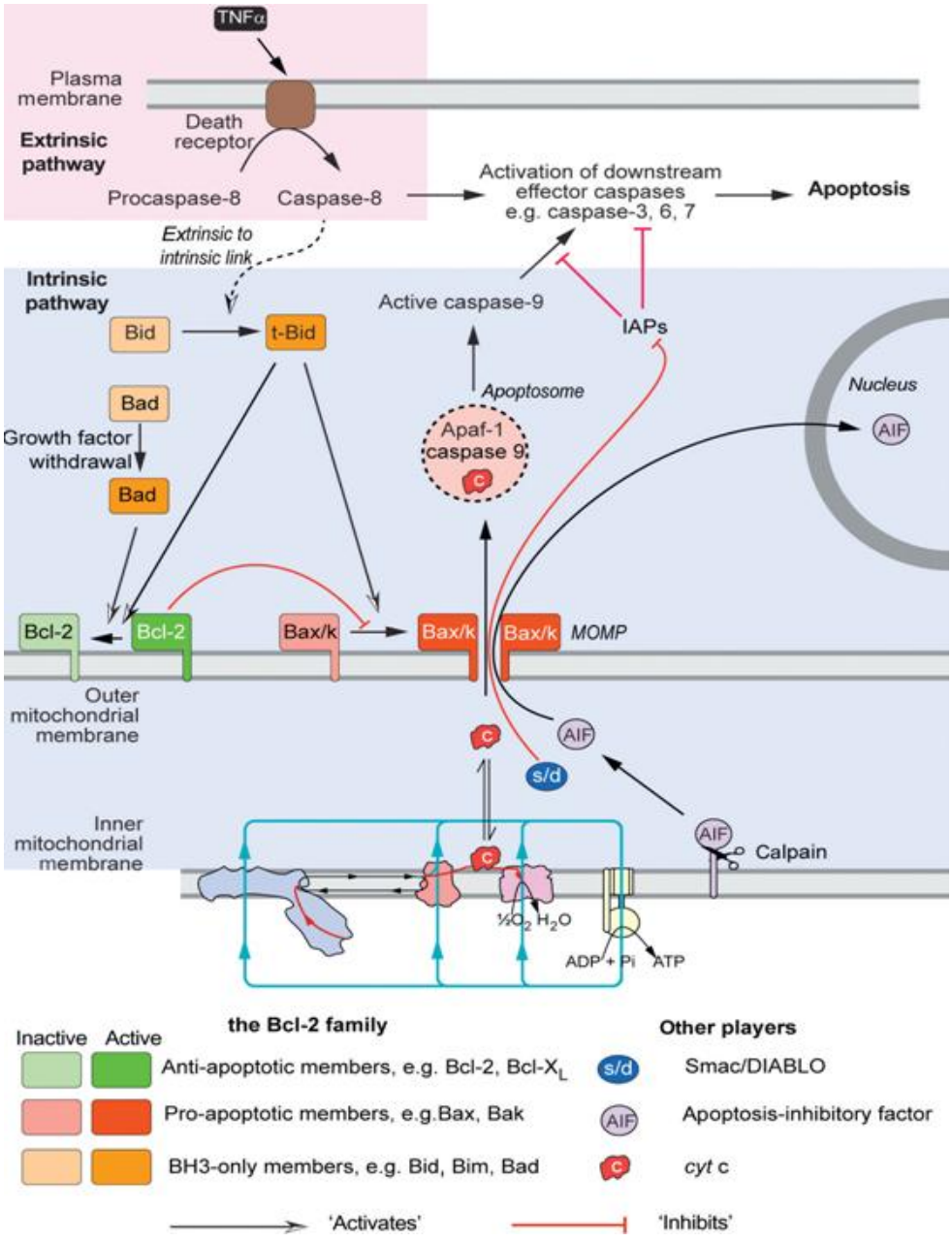

Figure 1.8- Schematic representation of extrinsic and intrinsic pathways of apoptosis. Apoptosis can result from the activation of two distinct molecular cascades, known as the extrinsic (or death receptor) and the intrinsic (or mitochondrial) pathways. Both pathways, which can converge at the level of mitochondria, involve the activation of initiator caspases (caspase-8 and -9, respectively) that catalyze the proteolytic maturation of downstream executioner caspases, such as caspase 3, which are the final effectors of cell death. Mitochondrial outer membrane permeabilization (MOMP) represents the point-of-no-return in the mitochondrial apoptotic pathway. Following MOMP, mitochondrial apoptogenic factors such as cytochrome *c*, Smac/Diablo or apoptosis inducing factor (AIF) are released to the cytosol. Once into the cytosol, these factors can initiate cell death in a caspase-dependent or a caspase-independent manner. MOMP is highly regulated by anti-apoptotic (e.g., Bcl-2 and Bcl-xL) and pro-apoptotic (e.g., Bax and Bak protein members of the Bcl-2 family) (from Nicholls & Fergunson, (2013)).

The formation of the mitochondrial outer membrane permeabilisation (MOMP) pore is an important feature of the intrinsic pathway. The pro-apoptotic proteins (Bax and Bak) attempt to undergo conformational changes, promoted by t-Bid and others BH_3 proteins, to form homo-oligomers that constitute the MOMP pore. t-Bid makes an important converging point of both apoptotic pathways since it is important in the intrinsic pathway and is activated by caspase-8 in the extrinsic pathway from the Bid protein.

Channel opening results in the loss of mitochondrial membrane potential ($\Delta\psi$) and allows the release from the mitochondrial intermembrane space of pro-apoptotic proteins including cytochrome *c*, Omi/HtrA2 (Omi stress-regulated endoprotease/High temperature requirement protein A 2), second mitochondria-derived activator (Smac/ Diablo) and apoptosis-inducing factor (AIF) (Soane et al., 2007). The released cytochrome c will form an apoptosome together with the apoptotic protease-activating factor-1 (Apaf-1) and dATP. Assembly of the apoptosome creates a platform that bring together procaspase 9, enabling their autoactivation which then activates the executioner caspase-3 (Ow et al., 2008). Omi/HtrA2 and Smac/Diablo will neutralize the inhibitory effect of cytoplasmic inhibitor of apoptosis proteins (IAPs) leading also to activation of caspases.

1.3 Silver Nanoparticles and Mitochondria

Once inside the body NPs can pass through cell membranes and interact with critical organelles such as mitochondria. Foley et al., (2002) demonstrated that NPs preferentially mobilize to mitochondria and may cause mitochondrial dysfunctions.

Few studies have been made so far regarding the effects of silver nanoparticles on mitochondria and most of them are made on *in vitro* models. One of the few studies carried out *ex vivo* demonstrated that silver nanoparticles affected the bioenergetic features of the mitochondria, decreasing the mitochondrial membrane potential and impairing the oxidative phosphorylation capacity (Teodoro et al., 2011).

As previously mentioned, Ag^{+} has high affinity for thiol groups present in the cysteine residues. Therefore AgNPs disturb the mitochondria through interaction with thiol groups of inner mitochondrial membrane proteins (Almofti et al., 2003). AgNPs may oxidate thiol groups of important cell membrane proteins, causing changes in membrane permeability and disrupts mitochondrial functions. For instance, silver ions can bind with transport proteins leading to proton leakage, resulting in collapse of the proton motive force (Marambio-Jones & Hoek, 2010). Hussain et al., (2005) shown reduced mitochondrial function and increasing membrane leakage of rat liver cells after silver nanoparticles.

AgNPs may affect mitochondria through impairments in ETC, causing ROS generation and affecting the production of ATP. As ATP is required for repair of DNA damages, reduction in its levels might impair energy-dependent DNA repair mechanisms (Asharani et al., 2009). Since the most of the mtDNA encodes for structural protein components of the ETC as well as two subunits of ATP synthase, damages on mtDNA have already been associated with defective electron transfer and ATP phosphorylation (Unfried et al., 2007).

Induction of the apoptotic process has been also related with effects of AgNPs on mitochondria. Some studies have shown that treatment of cells with AgNPs activate a mitochondria-dependent apoptotic pathway. Jing et al., (2011) reported that AgNPs induced loss of mitochondrial, which in turn leads to release of cytochrome *c*. This release initiates a cascade that leads to activation of caspase 9 and caspase 3, resulting in apoptosis. Activation of JNK was also present, and its inhibition through siRNA abolished cell death, suggesting that JNK is also involved in apoptotic process after AgNPs treatment. Another study of AgNPs toxicity carried out by Hsin et al., (2008)

suggested that apoptosis in fibroblast cells was mediated by a mitochondrial pathway. Generation of ROS by mitochondria activated apoptotic proteins, JNK and p53, which in turn induced Bax and consequently cytochrome *c* release. This enhancement of ROS production may cause oxidation of sulfhydryl groups of enzymes of the mitochondrial respiratory chain leading to mitochondrial dysfunction.

In conclusion, figure 1.9 shows a possible mechanism of AgNPs toxicity.

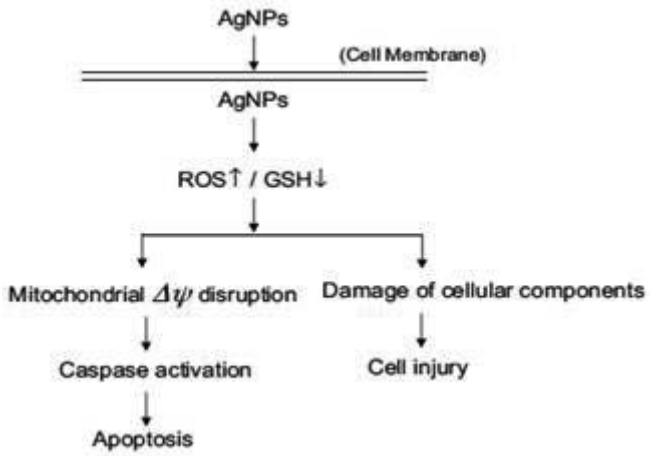

Figure 1.9- Possible mechanism of AgNPs toxicity. AgNPs can pass through cell membranes and interact with critical organelles such as mitochondria. Interaction with mitochondria may affect ETC, causing ROS generation and decrease GSH levels. The oxidative stress created might damage cellular components as well as lead to mitochondrial membrane permeability and disruption of mitochondrial functions. The loss of mitochondrial $\Delta\psi$ leads to release of cytochrome *c* and consequently activation of caspase 9 and caspase 3, resulting in apoptosis. (Image based on Jing et al., (2011)).

1.4 Objectives

The development of the nanotechnology industry has increased the number of products containing nanoparticles. Many people can get exposed chronically to these NPs in a variety of manners such as researchers manufacturing the NPs, patients injected with NPs, or people using products containing NPs. Although nanomaterials are widely used in modern technology, there is a severe lack of information about their possible effects in human health and environment. So far, most of the information about the mechanisms of AgNPs toxicity has been derived from *in vitro* studies. Just a few studies have been conducted *in vivo*, reflecting a significant gap of information about the increasing concern to the human health. More so, these *in vivo* studies have utilized rather high doses of AgNPs in an acute exposure time frame.

Thus, the main goal of this project is evaluate, *in vivo* and *ex vivo*, what are the consequences of AgNPs at low dose during a chronic exposure. We also intend to evaluate if, in these conditions, AgNPs interact with mitochondria, compromising its energetic functions. This approach can contribute to improve our knowledge about the mechanism by which AgNPs exert their toxicity, since this is the first time that AgNPs effects on mitochondria are evaluated at a low dose on a chronic exposure.

Since AgNPs exposure has been related with ROS generation, it will be assessed if chronic exposure can increase oxidative stress *in vivo* and whether this increase can be prevented by antioxidant administration. Finally, since the size of the nanoparticles is one of the features that makes them unique and alters their behavior when compared to their bulk chemical counterpart, we pretend elucidate the influence of particle size on AgNPs toxicity.

We expect that this work will contribute to improve our knowledge about the *in vivo* toxicity of AgNPs. In this way, allow help in delineating strategies to reduce or prevent this potential toxicity, taking into account that there is an exponential increase in the daily use of these NPs.

Chapter II

Materials and Methods

2.1 Materials and reagents

Citrate-coated spherical silver nanoparticles were acquired from Nanocomposix (www.nanocomposix.eu).

All other reagents and chemicals used were of the highest grade of purity commercially available.

2.2 Animals, diets and treatments

Male Sprague Dawley rats aged 10 weeks were purchased from Charles River Laboratories (France) and acclimated for 1 week before starting the experiments. They were housed under controlled light (12 h- light cycle) at 22 °C in a ventilated room. Food and water (pH 5.5) were supplied *ad libitum*. Animals were randomly selected and divided into 5 experimental groups (n=6 in each group):

1- control group (saline injected);

2- animals injected (once a week, during 1 month) with 250 µg/Kg AgNPs (size 10 nm);

3- animals injected (once a week, during 1 month) with 250 µg/Kg AgNPs (size 75 nm);

4- animals treated with N-acetylcysteine (100 mg/Kg) 30 minutes before injection (once a week, during 1 month) with 250 mg/Kg AgNPs (size 10 nm);

5- animals treated with N-acetylcysteine (100 mg/Kg) 30 minutes before injection (once a week, during 1 month) with 250 mg/Kg AgNPs (size 75 nm).

All animals were intraperitoneally (i.p.) injected.

All experimental procedures regarding the animals respected the institutional guidelines.

2. 3 Plasma biochemical determination

Blood samples were collected, before any animal treatment, by cutting the end of the tail. At the end of the study, animals were killed by decapitation and blood was again collected. Blood samples were mixed with EDTA and centrifuged at 2300 x*g* for

3 min. Plasma samples were collected and enzymatic determinations of alanine aminotransferase (ALT), aspartate aminotransferase (AST) and lactate dehydrogenase (LDH) performed using commercial kits.

2.4 Isolation of liver mitochondria

The animals were sacrificed by cervical dislocation and their liver was quickly removed. Liver was divided into 2 samples: for frozen tissue (immediately placed in liquid N_2, and stored at -80°C until analysis) and for preparation of mitochondria.

Hepatic tissue was finely minced in an ice-cold homogenization buffer (250 mM sucrose, 0.5 mM EGTA, 0.5% bovine serum albumin (BSA) and 10 mM HEPES, pH 7.4). The buffer was renewed several times to remove excess of blood. Then, the tissue was homogenized with a "Potter-Elvejhem" type glass homogenizer and a Teflon piston (Figure 2.1).

Mitochondria were isolated from the liver by differential centrifugation, as previously described (Rolo et al., 2009). Briefly, the homogenate was centrifuged (Sigma 3-18K Centrifuge) at 500 x*g* for 10 min at 4°C. This centrifugation was made to remove the heavier compounds in the homogenate (nucleus, cell fragments). Supernatant was collected and centrifuged at 10,000 x*g* for 10 min at 4°C to pellet mitochondria. Mitochondrial fraction was resuspended, using a brush, in a washing medium (250 mM sucrose and 10 mM HEPES, pH 7.4) and again centrifuged in the same condition. Mitochondria in the pellet were resuspensed in a final washing medium and immediately used. All operations were performed on ice during the isolation procedure.

1. Homogenization

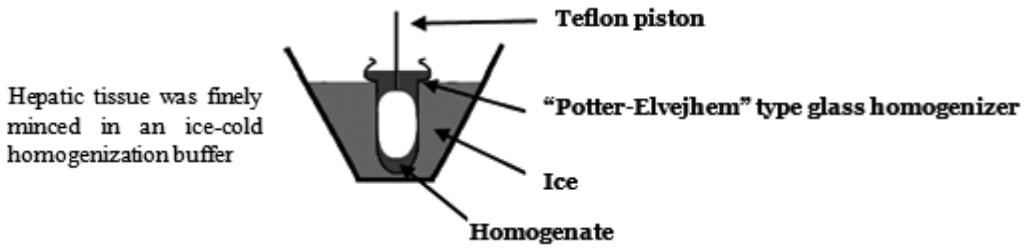

2. Differential centrifugation

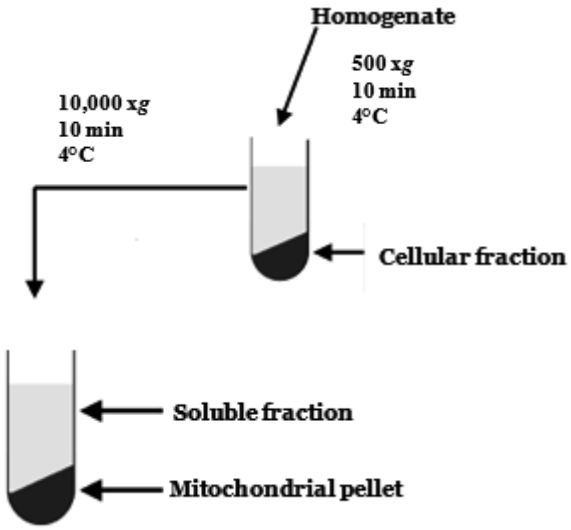

3. Washing and purification

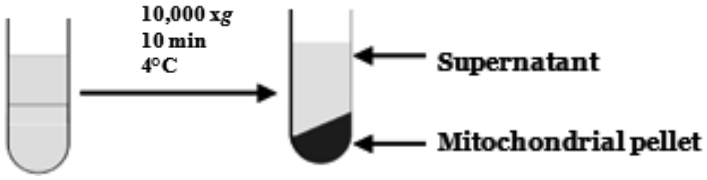

Figure 2.1- Schematic representation of liver mitochondria isolation.

2.5 Determination of protein concentration

Protein concentration in mitochondrial preparation was determined by the biuret method (Gornall et al., 1949). A standard curve was prepared by dilution series of BSA (0; 1; 1.5 and 2 mg/mL) from 0.4% stock, H_2O was added so that, together with BSA, the final volume was 0.5 mL. 50 µL of wash medium, 50 µL of DOC and 2 mL of biuret reagent were also added.

Mitochondrial preparations (50 µL) were mixed with 50 µL of deoxycholate (DOC) (10%) to help protein solubilization. The amount of water to make a final volume of 0.5 mL was added and then, 2 mL of biuret reagent. The standard curve and samples were

vortexed and placed at 37°C and allow to react for 10 minutes. Then, the samples and standard curve were transferred to cuvettes and the absorbance was measured at 540 nm, using a Heλios spectrophotometer (ThermoElectronCorporation).

2.6 Mitochondrial membrane potential measurements

Mitochondrial membrane potential ($\Delta\psi$) was estimated using an ion-selective electrode to measure the distribution of tetraphenylphosphonium (TPP^+) according to previously established methods (Kamo et al., 1979), and using an Ag/AgCl electrode as reference. The entrance of TPP^+ in mitochondria was determined by TPP^+ concentration decreasing in the medium, measured by electrode potential (Figure 2.2).

The potential difference generated between the selective electrode and the reference was measured with a Jenway electrometer (model 3305) and the output signal to a Kipp & Zonen recorder, after passing by a compensation circuit voltage basal (Madeira, 1975).

The TPP^+ equilibrates passively across biological membranes until electrochemical equilibrium is reached, thus $\Delta\psi$ can be estimated from the following equation (at 25°C):

$$\Delta\psi \text{ (mV)} = 59 \log (v/V) - 59 \log (10^{\Delta E/59} - 1),$$

where v, V and E are mitochondrial volume, volume of the incubation medium, and deflection of the electrode potential from the baseline, respectively (Palmeira & Rolo, 2012). A matrix volume of 1.1 µL/mg protein was assumed.

Briefly, mitochondria (1mg) were suspended in an open chamber with constant stirring, at 25°C, in 1.3 mL of respiratory buffer (130 mM sucrose, 50 mM KCl, 5 mM $MgCl_2$, 5 mM KH_2PO_4, 50 µM EDTA, 5 mM HEPES, pH 7.4) supplemented with 3 µM TPP^+. This TPP^+ concentration was used to achieve high sensitivity in measurements and to avoid possible toxic effects on mitochondria. Reactions were initiated by energizing mitochondria by adding 5 mM succinate. To avoid Complex I contribution due to possible endogenous substrates were added 3 µM of rotenone, a Complex I inhibitor. After the steady-state distribution of TPP^+ occurred, ADP (200 nmol) was added to initiate the phosphorylative cycle.

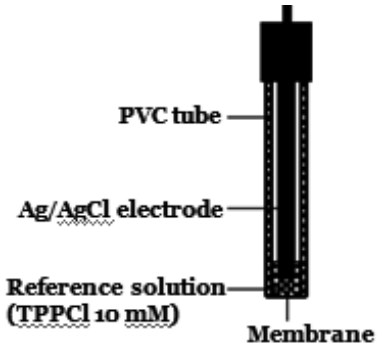

Figure 2.2- TPP electrode. Membrane potentials are measured with a TPP^+ electrode constructed by the use of a polyvinylchloride-based membrane containing tetraphenylboron as an ion-exchanger.

2.7 Mitochondrial Respiration

Oxygen consumption of isolated mitochondria was polarographically determined with a Clark oxygen electrode, as previously described (Rolo et al., 2009). Clark oxygen electrode, although only determines directly the rate of the final transfer of electrons to O_2, provides a lot of information about mitochondrial processes by the simple arrangement of the incubation conditions. Substrate dehydrogenase activity, respiratory chain activity, adenine nucleotide transport across the membrane, ATP synthase activity, and H^+ permeability of the membrane are some examples are the mitochondrial processes that might be investigated using the Clark oxygen electrode (Nicholls & Fergunson, 2013). The Clark oxygen electrode consists of two electrodes (platinum cathode and silver anode) immersed in the electrolyte (KCl) (Figure 2.3). O_2 is reduced to H_2O at the Pt electrode, which is maintained 0.7V negative with respect to the Ag/Cl reference electrode. The current flow is proportional to the O_2 concentration in the medium.

When KCl is the electrolyte occurs the following reactions:

Reaction 1: $Ag \rightarrow Ag^+ + e^-$

$\downarrow$

$Ag^+ + Cl^- \rightarrow AgCl$

Reaction 2: $O_2 + 2H_2O + 2e^- \rightarrow H_2O_2 + OH^-$

$\downarrow$

$H_2O_2 + 2e^- \rightarrow 2OH^-$

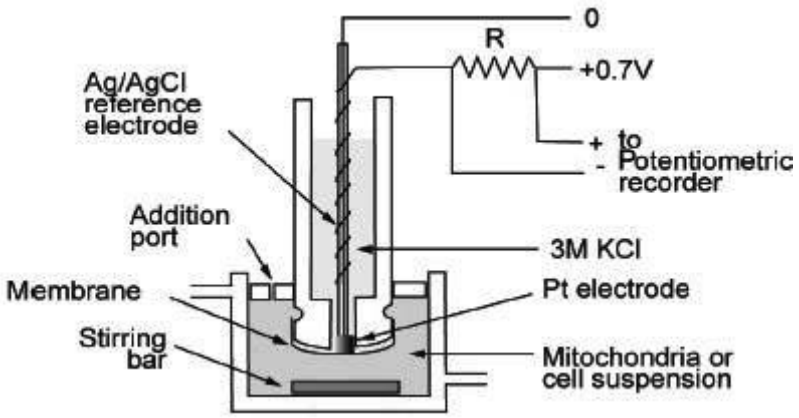

Figure 2.3- The Clark oxygen electrode. This electrode records the current flowing between the platinum electrode and the silver reference electrode held 0.7V positive. The current is proportional to the oxygen tension. (Nicholls & Fergunson, 2013)

Briefly, 1 mg of mitochondria was placed in an open chamber with constant stirring, at 25°C, in 1.3mL of the respiration buffer (as above) with rotenone (3µM) and succinate (5mM).

The respiratory state 3 was initiated by the addition of ADP (200 nmol). After the phosphorylation of the ADP to ATP, respiratory rate became slower (state 4). The respiratory control ratio (RCR) was calculated by the ratio between the state 3 and the state 4 respirations and used as a parameter of mitochondrial integrity.

The ADP/O ratio was calculated by the ratio between the amount of ADP added and the O_2 consumed during the state 3 respiration, as previously reported by Chance & Williams (1956).

Respiration in the presence of oligomycin was induced by the addition of ADP (200 nmol) and oligomycin (1 µg/mg protein) to evaluate the proton leak through the inner mitochondrial membrane. Oligomycin is specific inhibitor of ATPase, which creates a non-phosphorylative respiration.

Carbonyl cyanide 4-(trifluormethoxy) phenylhydrazone (FCCP)-uncoupled respiration was promoted by the addition of FCCP (1 µM). FCCP is an ionophore that uncouples oxidative phosphorylation by inducing artificial proton permeability in the mitochondria, stimulating the maximum respiration rate.

2.8 Succinate dehydrogenase activity

Succinate dehydrogenase (SDH) (Complex II of electron transport chain) of activity was polarographically determined as previously described (Singer, 1974). The reaction was carried out in a chamber sealed, except for a small addition port, at 25 °C in 1.4 mL of standard respiratory medium (as in mitochondrial respiration) supplemented with 5mM succinate, 2 μM rotenone, 0.1 μg antimycin A, 1mM KCN and 0.3 mg Triton X-100. Rotenone, antimycin A and KCN were added to inhibit complexes I, III and IV, respectively. Thus, SDH is the only mitochondrial respiratory complex working in the ETC, being the oxygen consumption directly related with SDH activity.

After the addition of freeze–thawed mitochondria (0.5 mg), 1 mM phenazinemetosulphate (PMS) was added to allow the initiation of the reaction. PMS is an intermediate electron acceptor which accepts electrons from SDH and transfers them to oxygen. Thus, the oxygen is reduced to H_2O and the consequent decrease of oxygen concentration is detected by the Clark oxygen electrode.

2.9 Cytochrome c oxidase (COX) activity

COX activity was polarographically determined with a Clark oxygen electrode, as previously described (Brautigan et al., 1978; Varela et al., 2008). The reaction was carried out in a chamber sealed, except for a small addition port, at 25 °C in 1.4 mL of standard respiratory medium (as in mitochondrial respiration) supplemented with 2μM rotenone, 10 μM oxidized cytochrome *c* and 0.3 mg Triton X-100. After the addition of freeze–thawed mitochondria (0.5 mg), 5mM ascorbate plus 0.25mM tetramethylphenylene-diamine (TMPD) was added to allow the initiation of the reaction. Ascorbate is added as the reductant to regenerate TMPD from its oxidized form. TMPD donates electrons to the respiratory chain via cytochrome *c*. Cytochrome *c*, is mobile protein from the intermembrane space, which will reduce cytochrome *c* oxidase (Complex IV). Here, the electrons are transferred to the final electron acceptor, molecular oxygen (O_2), generating H_2O. The decrease of oxygen concentration is measured using the Clark oxygen electrode.

2.10 ATPase activity

ATPase activity of the mitochondrial ATP synthase was spectrophotometrically determined at 660 nm, in association with ATP hydrolysis (Varela et al., 2008). The ATP synthase is a reversible enzyme that only runs in the direction of ATP synthesis by the continual regeneration of proton motive force (Δp) and the use of ATP by the cell. However, when this Δp is depressed, ATP synthase works as an ATPase, generating a Δp similar to that produce by the respiratory chain. The ATP hydrolysis yields inorganic phosphate (Pi), which can be measured by a simple colorimetric reaction. The amount of Pi produced by ATP hydrolysis is directly proportional to the activity of ATPase and was determined at 660 nm using a Heλios spectrophotometer (ThermoElectronCorporation).

Briefly, the reaction was carried out at 37°C, in 2 mL of reaction medium (125 mM Sucrose, 65 mM KCl, 2.5 mM $MgCl_2$, and 50 mM HEPES, pH 7.4). Mitochondria (0.25 mg) were added to reaction medium and the reaction was initiated by addition 2 mM Mg^{2+}-ATP, in the presence or absence of oligomycin (1 µg/mg protein). After 10 min, the reaction was stopped by adding 1 ml of 40% trichloroacetic acid. 2 mL of ammonium molybdate (1%) plus 2 mL H_2O were then added to 1 ml of reaction volume and reacted for 5 min at room temperature. ATPase activity was calculated as the difference in total absorbance and absorbance in the presence of oligomycin.

2.11 Determination of ATP content

Adenosine nucleotide extraction was performed as follows. Tissue samples were pulverized with a mortar and pestle in liquid N_2 and homogenized in ice-cold KOH buffer (KOH 2.5M, K_2HPO_4 1.5 M), H_2O, K_2HPO_4 1 M on ice. pH was adjusted to 7 with HCl 1M and samples were vortexed and centrifuged at 18 000 x*g* for 2 min, at 4 ºC. The supernatants were collected and frozen at -80 ºC for posterior use. Adenosine nucleotides were quantified with an ATP bioluminescent assay kit (Sigma- Aldrich) on a Victor^3 plate reader.

2.12 Evaluation of reactive oxygen species (ROS) generation

ROS production was determined fluorometrically using a Perkin-Elmer VICTOR^3 plate reader fluorometer (Zhou et al., 2001). 2',7'-dichlorodihydrofluorescein diacetate (H_2DCFDA) is a nonfluorescent probe which easily crosses the cell membrane and once within the cell, the acetate groups are removed by intracellular esterases. Upon oxidization by ROS, the nonfluorescent H_2DCFDA is converted to the highly fluorescent 2′,7′-dichlorofluorescein (DCF). DCF has an excitation wavelength of 485 nm and an emission wavelength of 538 nm, and thus it can be detected using a fluorometer. Therefore, the fluorescence emitted by DCF is used as an indicator of reactive oxygen species (ROS) generation.

Briefly, isolated mitochondria (1 mg/ml) were suspended in standard respiratory médium (130 mM sucrose, 50 mM KCl, 5 mM MgCl2, 5 mM KH2PO4, 50 μM EDTA, 5 mM HEPES (pH 7.4), and 3 μM rotenone) loaded with 50 μM H_2DCFDA (in DMSO) for 15 min at 25ºC. After incubation, the samples were spun at 3000 rpm for 3 min and the resultant pellet was suspended in medium. 200 μl of the mitochondrial suspension were loaded into a 96-well plate and the fluorescence monitored. After basal fluorescence measurement, antimycin A was added to all preparation to block complex III of the mitochondrial chain, to induce maximal ROS generation. The results were expressed as relative fluorescence units (RFUs).

2.13 Mitochondrial permeability transition (MPT)

Mitochondrial swelling was estimated by changes in light scattering, as spectrophotometrically monitored in a Heλios spectrophotometer (ThermoElectronCorporation) at 540 nm (Palmeira and Wallace, 1997). The experiments were started by the addition of mitochondria (1 mg) to a final volume of 2 mL of the standard incubation medium (200 mM sucrose, 10 mM HEPES (pH 7.4), 1 mM KH_2PO_4 and 10 μM EGTA) supplemented with 3 μM rotenone and 5 mM succinate and, in selected assays, Cyclosporin A 1 μM, a known mPT inhibitor as a negative control. The reaction temperature was maintained at 25ºC. After a brief incubation period to establish a baseline absorbance, different calcium concentrations were added as indicated by the arrows in the figure, to induce permeability transition.

2.14 Western Blotting analysis

The mitochondrial content of COX-I, COX-IV and tubulin were determined by western blotting. Tissue samples were pulverized with a mortar and pestle in liquid N_2 and homogenized in ice-cold lysis buffer supplemented with a protease inhibitor. Equal amounts of protein (50 µg) were mixed with Laemmli sample buffer and heat-denaturation was performed immediately prior to one-dimensional gel electrophoresis. Proteins were separeted on 15% SDS-polyacrylamide gel, using a Mini-Protean electrophoresis system (Bio-Rad Laboratories, Inc., CA, EUA) for 90 minutes, 100 V, with electrophoresis buffer (25 mM Tris, 192 mM glycine, 0.1% SDS, pH 8.3)

The proteins were transferred to polyvinylidene difluoride (PVDF) membrane for 90 minutes, 100 V, using transfer buffer (25mM Tris, 192 mM glycine, 20% methanol, pH 8.3), under magnetic stirring. The transfer occurred in Mini Trans-Blot (Bio-Rad Laboratories, Inc., CA, EUA) placed in ice.

Membranes were blocked in TBS (25 mM Tris-HCl (pH 7.6) and 150 mM NaCl) supplement with 5% nonfat milk for 2 hours. After the blockage, membranes were washed with TBS-T (TBS supplement with Tween-20 1%) and then, incubated with anti-COX I (1:100), anti-COX IV (1:1000) or anti-tubulin (1:5000) overnight at 4ºC with gentle shaking. Immunodetection was performed with Western-Dot 625 (Invitrogen) goat anti-rabbit or goat anti-mouse western blot kits. Membranes were imaged using a Gel Doc instrument (Biorad) and the densitometric analysis was performed with the ImageJ software.

Table II- List of utilized antibodies for Western blot, source and utilized dilution.

Antibody	Specie	Dilution	Supplier	Reference
Tubulin	Rabbit	1:5000	Abcam	ab52866
COX-I	Mouse	1:100	MitoSciences	MS404
COX-IV	Mouse	1:1000	MitoSciences	MS407

2.15 Statistic analyses

Data are presented as mean ± S.E.M. Statistical significance was determined using one way ANOVA followed by Bonferroni post-hoc test. A value of $p<0.05$ was considered as statistically significant.

Chapter III

Results

3.1 Food consumption and effect on body weight

In order to evaluate the effect of AgNPs administration in terms of food consumption and body weight gain, the food intake as well as the animals weights were measured once a week.

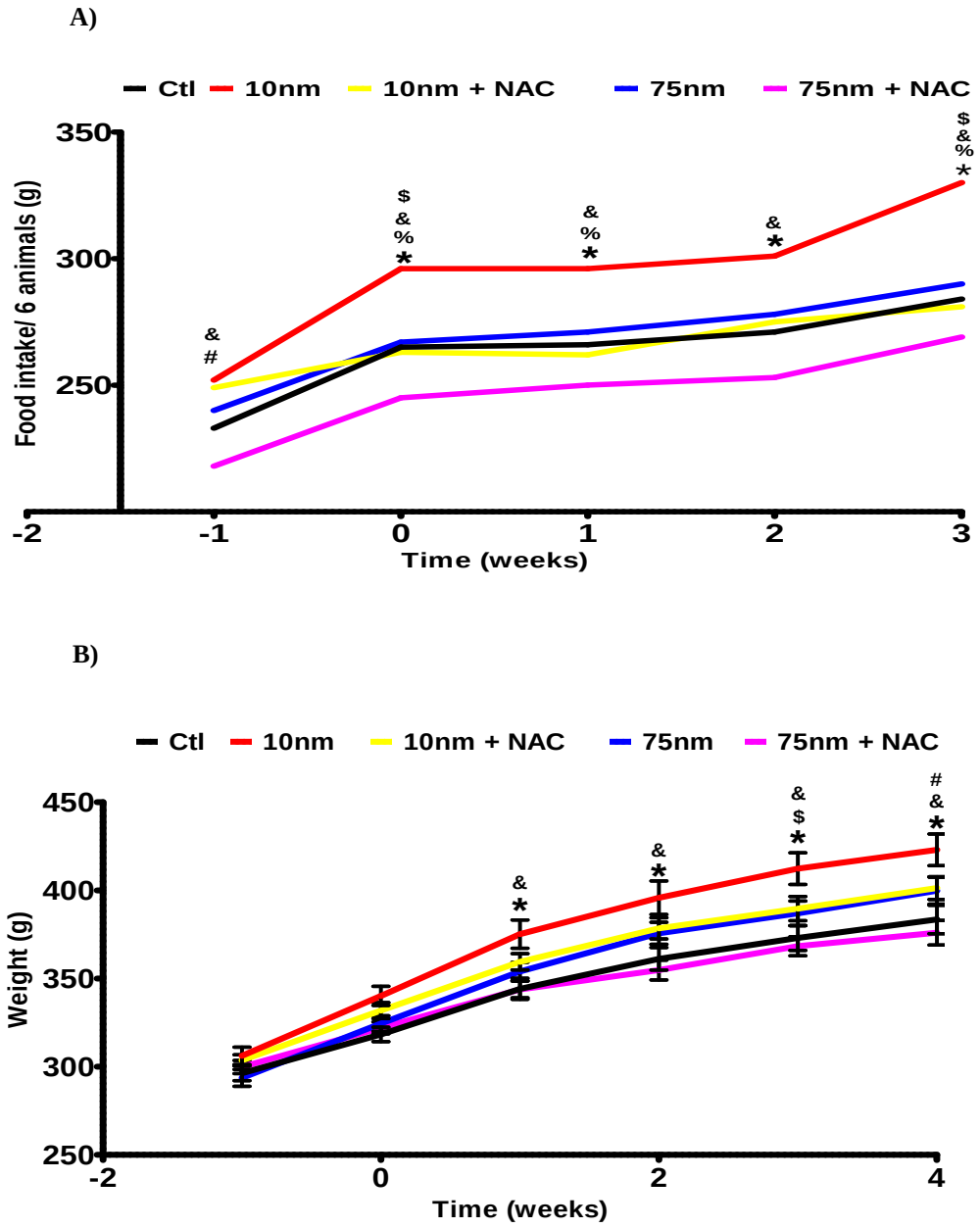

Figure 3.1- Food intake (A) and animal total body weight progression (B) throughout the study. Data are means ± S.E.M of experiments performed with six animals/group(p<0.05).* indicates statistically significant difference between 10 nm and control; & indicates statistically significant difference between 10 nm and 75 nm+NAC; $ indicates statistically significant difference between 10nm and 75 nm; # indicates statistically significant difference between 10nm+NAC and 75 nm+NAC; % indicates statistically significant difference between 10 nm and 10 nm+NAC.

As can be seen in Figure 3.1 A, the food intake of 10nm-AgNPs group was significantly higher than the others experimental groups throughout the study even before the nanoparticles administration. Regarding body weight progression, 10nm-AgNPs group showed a significant increase after the first week until the end of the experiment (Fig.3.1 B)

3.2 Plasma markers of liver injury

To determine if silver nanoparticles induced liver injury, serum levels of ALT, AST and LDH were evaluated. As shown in Figure 3.2 A and B, all groups significantly increased plasma ALT and AST levels after 4 weeks of treatment (T4) compared to the begin of the experiment, before any treatment (T0). Administration of NAC was effective in reducing the increase in plasma levels of AST caused by 10nm-AgNPs on T4. Plasma LDH levels were also significantly increased on T4 in groups with both sizes of silver nanoparticles compared to T0. Administration of NAC was effective in reducing the increase in plasma levels of LDH caused by 75nm-AgNPs on T4.

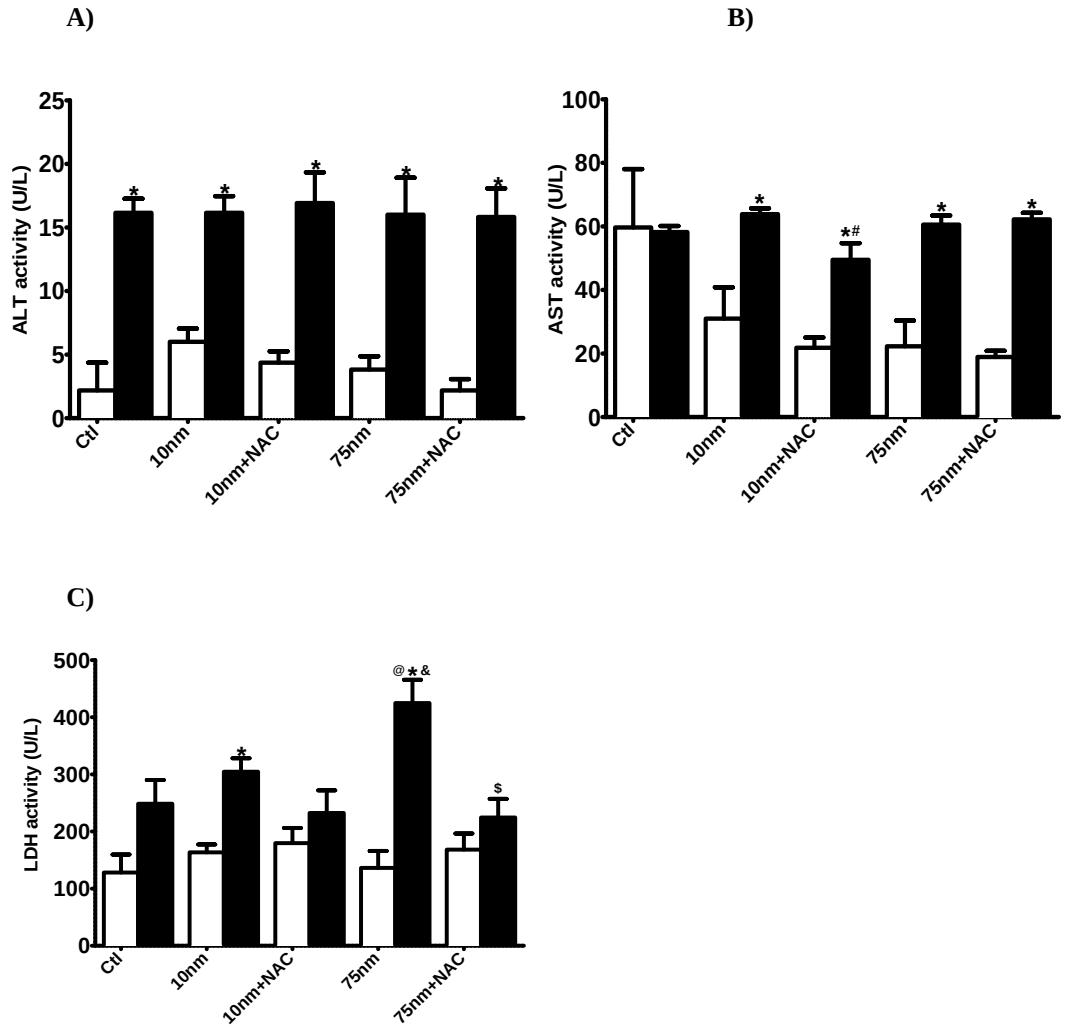

Figure 3.2- The effect of silver nanoparticles on plasma levels of (A) alanine aminotransferase (ALT), (B) aspartate aminotransferase (AST) and (C) lactate dehydrogenase (LDH). Plasma samples were collected and enzymatic determinations of ALT, AST and LDH performed using commercial kits. White columns represent plasma collected in the beginning of the study, before any administration (T0). Black columns represent plasma collected at the end of the study, after all administrations (T4). Data are means ± S.E.M of experiments performed with five animals/group(p<0.05). *indicates statistically significant difference between white and black columns in the same experimental group; # indicates statistically significant difference between 10 nm and 10 nm+NAC @ indicates statistically significant difference between 75 nm and control; & indicates statistically significant difference between 75 nm and 10nm+NAC; $ indicates statistically significant difference between 75 nm+NAC and 75 nm.

3.3 Mitochondrial membrane potential

Membrane potential (Δψ) sustained by mitochondria is fundamental for mitochondrial function. Results are summarized in Table III.

Table III- Effects of silver nanoparticles in mitochondrial membrane potential. Mitochondrial membrane potential (Δψ) determined in the presence of succinate as respiratory substrate. Reactions were carried out in 1.3 mL of reaction medium, supplemented with 3 µM rotenone and 1 mg of freshly isolated mitochondria, as described in Materials and Methods chapter. Data are means ± SEM of experiments performed with six different mitochondrial preparations(p<0.05). *indicates statistically significant difference versus control; # indicates statistically significant difference versus 10 nm; $ indicates statistically significant difference versus 75 nm.

	Control	**10 nm**	**10 nm + NAC**	**75 nm**	**75 nm + NAC**
Initial Δψ (-mV)	216.20 ± 2.20	197.50 ± 3.77 *	212.30 ± 0.96#	205.00 ± 1.20*	214.60 ± 0.55#$
Δψ Depolarization (-mV)	30.16 ± 0.71	23.61 ± 0.71*	26.76 ± 0.40	25.78 ± 0.89*	29.10 ± 1.05#
Δψ Repolarization (-mV)	214.90 ± 2.25	191.20 ± 3.60*	209.50 ± 1.13#	201.80 ± 1.26*#	211.40 ± 0.55#$

Δψ significant decreased in mitochondria exposed to either 10- or 75-nm AgNPs (Table III). A significantly alteration was seen in 75nm+NAC group when compared to 10- and 75 nm. Depolarization induced by the addition of ADP and Δψ after repolarization (mitochondrial capacity to establish Δψ after ADP phosphorylation) also decreased in mitochondria exposed to both sizes of AgNPs.

When pretreated with NAC, the mitochondria showed a significantly higher mitochondrial Δψ after repolarization when compared with the same conditions without NAC. Another important difference regarding mitochondrial Δψ after repolarization was seen between both AgNPs sizes. 75nm- was significantly higher than 10nm-AgNPs.

Finally, the lag phase (time necessary for ADP phosphorylation) was significantly longer in the presence of both sizes of AgNPs, illustrating a clear impairment of mitochondrial function (Figure 3.3). Once again, NAC was able to combat such effect.

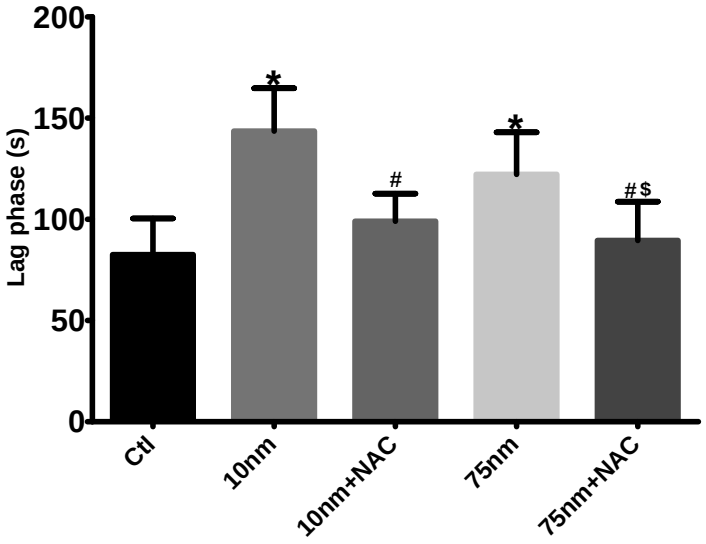

Figure 3.3- Effects of silver nanoparticles in the lag phase preceding the mitochondrial repolarization. Mitochondrial lag phase was performed with the TPP^+-selective electrode. Data are means ± SEM of experiments performed with six different mitochondrial preparations($p<0.05$). *indicates statistically significant difference versus control; # indicates statistically significant difference versus 10 nm; $ indicates statistically significant difference versus 75 nm.

3.4 Mitochondrial respiration/oxygen consumption

The possible alterations caused by AgNPs in oxidative phosphorylation and respiratory chain were investigated. Mitochondrial state 3 respiration (ADP-induced oxygen consumption) was significantly decreased in mitochondria exposed either size of silver nanoparticles, an effect reversed by NAC (Table IV). The consumption of oxygen after ADP phosphorylation (state 4 respiration) was slightly increased in mitochondria exposed to 10nm-AgNPs and significantly increased with 75nm-AgNPs. However, in the presence of NAC, state 4 respiration of 75nm-AgNPs group was significantly decreased. Consequently, the ratio between state 3 and state 4 respiration (RCR), was significantly decreased in mitochondria exposed to either size of AgNPs. The ADP/O ratio, an indicator of oxidative phosphorylation efficiency, showed a significantly decrease when mitochondria were exposed to either AgNPs sizes. However, once again NAC significantly reverted this effect.

Table IV- Oxygen consumption measurements. State 3 respiration, state 4 respiration, respiratory control ratio (RCR), ADP/O, Oligomycin-inhibited oxygen consumption (v Oligomycin) and FCCP-stimulated oxygen consumption (v FCCP) in liver mitochondria, upon incubation with silver nanoparticles. Reactions were carried out in 1.3 mL of reaction medium, supplemented with 3 µM rotenone and 1 mg of freshly isolated mitochondria, as described in Materials and Methods chapter. Data are means ± SEM of different experiments performed with six different mitochondrial preparations($p<0.05$). *indicates statistically significant difference versus control; # indicates statistically significant difference versus 10 nm; $ indicates statistically significant difference versus 75 nm; & indicates statistically significant difference versus 10nm+NAC.

	Control	**10 nm**	**10 nm + NAC**	**75 nm**	**75 nm + NAC**
State 3 (nAtoms O/min/mg protein)	151.5 ± 12,75	85.1 ± 5.65*	120.2 ± 9.01#	92.87± 7.14*	151.1 ± 7.89#$
State 4 (nAtoms O/min/mg protein)	34.7 ± 1.37	44.8 ± 2.26	41.73 ± 4.45	54.46± 5.26*	39.16 ± 2.76$
RCR	3.35 ± 0.28	2.17 ± 0.08*	2.675 ± 0.38	2.153± 0.19*	3.293 ± 0.09#$
ADP/O	1.75 ± 0.012	1.22 ± 0.039*	1.49 ± 0.029#	1.18 ± 0.024*&	1,58 ± 0,082#$
v Oligomycin (nAtoms O/min/mg protein)	33.57 ± 4.06	57.1 ± 4.87*	51.97 ± 1.60*	61.93± 3.72*	41.00 ± 2.62#$
v FCCP (nAtoms O/min/mg protein)	259.1 ± 12.13	109.8± 3.29*	202.3 ± 20.7*#	140.4 ± 10.14*&	204.7 ± 9.86*#$

Mitochondrial respiration under non-phosphorylative conditions was also evaluated in the presence of oligomycin, a specific inhibitor of ATP synthase. Mitochondria exposed to either size of silver nanoparticles were significantly increased when compared to control. 75nm+NAC group was significantly lower when compared to the same condition without NAC (75nm group).

Oxygen consumption was stimulated by v FCCP, a well-known respiratory chain uncoupler. The results show a significant decrease in all experimental groups when compared to control. However, the presence of NAC prevented AgNPs deleterious action, shown by the significant increase in the FCCP-uncoupled respiration.

3.5 ATPase activity

The enlarged lag phase in mitochondria exposed to AgNPs suggested that this exposure could affect ATPase, a key component of the phosphorylative system. In order to clarify this alteration, mitochondrial ATPase activity was evaluated (Fig.3.4). Both mitochondria ATPase activity exposed to either size of silver nanoparticles were significantly decreased when compared to control. 75nm+NAC group showed values of ATPase activity similar to the control group suggesting that NAC prevented AgNPs deleterious action against ATPase.

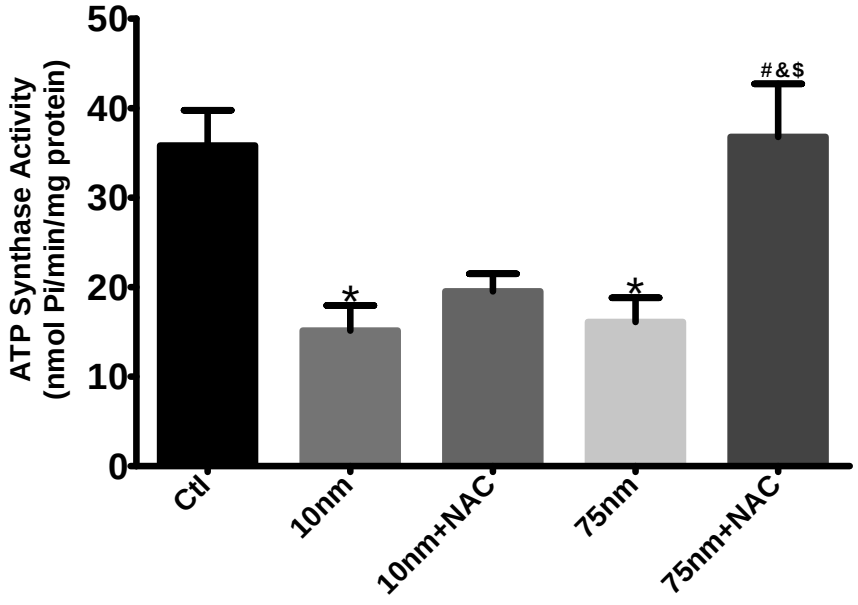

Figure 3.4- ATPase activity in liver mitochondria. ATPase activity was spectrophotometrically determined at 660 nm and was calculated as the difference in total activity and activity in the presence of oligomycin. Data are means ± S.E.M of experiments performed with six animals/group(p<0.05). *indicates statistically significant difference versus control; # indicates statistically significant difference versus 10 nm; $ indicates statistically significant difference versus 75 nm; & indicates statistically significant difference versus 10nm+NAC

3.6 Adenine nucleotides content

The decreased ATPase activity in mitochondria isolated from animals injected with both AgNPs sizes may suggest problems in ATP phosphorylation. To further determine whether AgNPs affect mitochondrial ATP production, endogenous ATP content was evaluated. As can be seen in Figure 3.5, both AgNPs sizes showed value similar to the control group. However, in the presence of NAC, ATP content levels tend to be slightly higher.

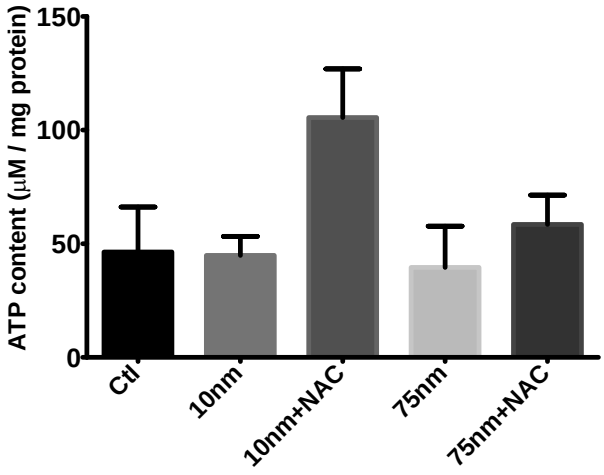

Figure 3.5- The effect of silver nanoparticles on ATP content. ATP content was evaluated by using a bioluminescent assay kit as described on Materials and Methods chapter. Data are means ± S.E.M of experiments performed with five animals/group.

3.7 Enzymatic activities

The decreased rate of oxygen consumption induced by FCCP in mitochondria isolated from animals injected with either size of AgNPs suggested alterations in the mitochondrial electron transport chain complexes. In view of this, succinate dehydrogenase (SDH) and cytochrome *c* oxidase (COX) activities were evaluated.

As expected, both AgNPs sizes exhibited significantly decreased activities in SDH when compared to control (Fig.3.6 A). NAC was able to significantly increase this enzyme activity in the presence of 75nm-AgNPs.

COX activity significantly decreased in mitochondria exposed to 75nm-AgNPs comparing to control. This effect was recovered in the presence of NAC (Fig.3.6 B). The administration of 10nm-AgNPs showed a slight decrease when compared to control, which was significantly recovered in the presence of NAC.

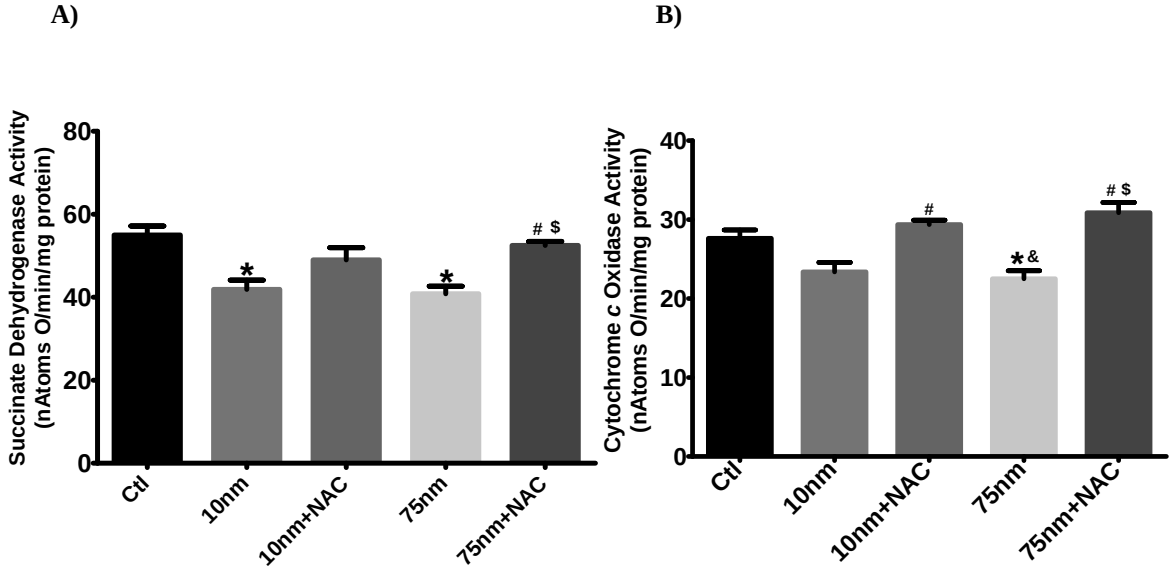

Figure 3.6- (A) Succinate dehydrogenase activity; (B) Cytochrome *c* oxidase activity in liver mitochondria incubated with silver nanoparticles. Enzyme activity was polarographically measured using a Clark oxygen electrode as described in Materials and Methods chapter. Data are means ± S.E.M of experiments performed with six animals/group(p<0.05). *indicates statistically significant difference versus control; # indicates statistically significant difference versus 10 nm; $ indicates statistically significant difference versus 75 nm; & indicates statistically significant difference versus 10nm+NAC.

3.8 Generation of reactive oxygen species (ROS)

Both *in vivo* and *in vitro* studies have shown that AgNPs lead to ROS production (Arora et al., 2008; Carlson et al., 2008; Ghosh et al., 2012; Tiwari et al., 2011). In order to assess if our data also shown a similar effect, the evaluation of the ROS production in mitochondria exposed to AgNPs was performed.

For both AgNPs sizes tested, ROS production rate was significantly increased when compared to the control group, either in the presence or absence of antimycin A (Fig. 3.7). Mitochondria isolated from the livers exposed to NAC revealed statistically non-significant trend towards decreased ROS production in both sizes of AgNPs.

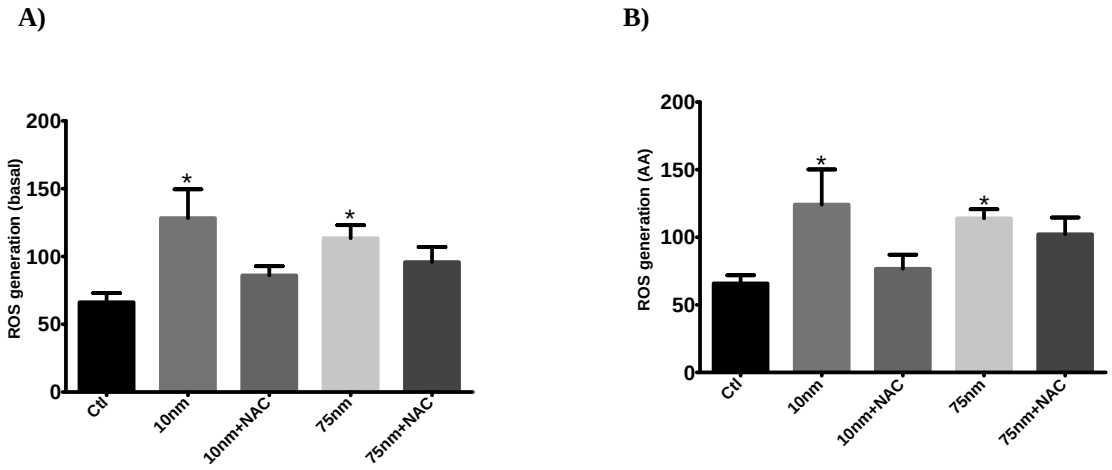

Figure 3.7- The effects of silver nanoparticles on reactive oxygen species (ROS) generation. ROS were estimated fluorometrically using the probe H_2DFDA, as described in Materials and Methods chapter. A) After basal fluorescence measurement, Antimycin A was added to all preparations (B) to block complex III of mitochondrial respiratory chain, and so to induce heightened ROS generation. Data are means ± S.E.M of experiments performed with six animals/group(p<0.05). *indicates statistically significant difference versus control.

3.9 Mitochondrial permeability transition

Mitochondrial calcium retention capacity is an important component of mitochondrial function. Although the ability of mitochondria to accumulate Ca^{2+} is somewhat high, it is not infinite (Chalmers & Nicholls, 2003). Mitochondria show a finite capacity of accumulating calcium and, after a certain threshold, undergo the mitochondrial permeability transition (MPT), possibly through the formation of a multichannel pore (Rasola & Bernardi, 2011). Several factors can induce MPT, such as increased ROS generation, decreased ATP content and high calcium concentration. This threshold varies, in accordance with several mitochondrial parameters, as the mitochondria's membrane potential, among others. The simplest way to observe the MPT with isolated mitochondria is to follow the decrease in light scattering of the suspension as the mitochondrial matrix swells and the outer membrane ruptures. The faster the decrease in absorption, the worse the mitochondrial calcium retention capacity. As such, the amount of calcium mitochondria can accumulate and for how long is an extremely useful indicator of mitochondrial function.

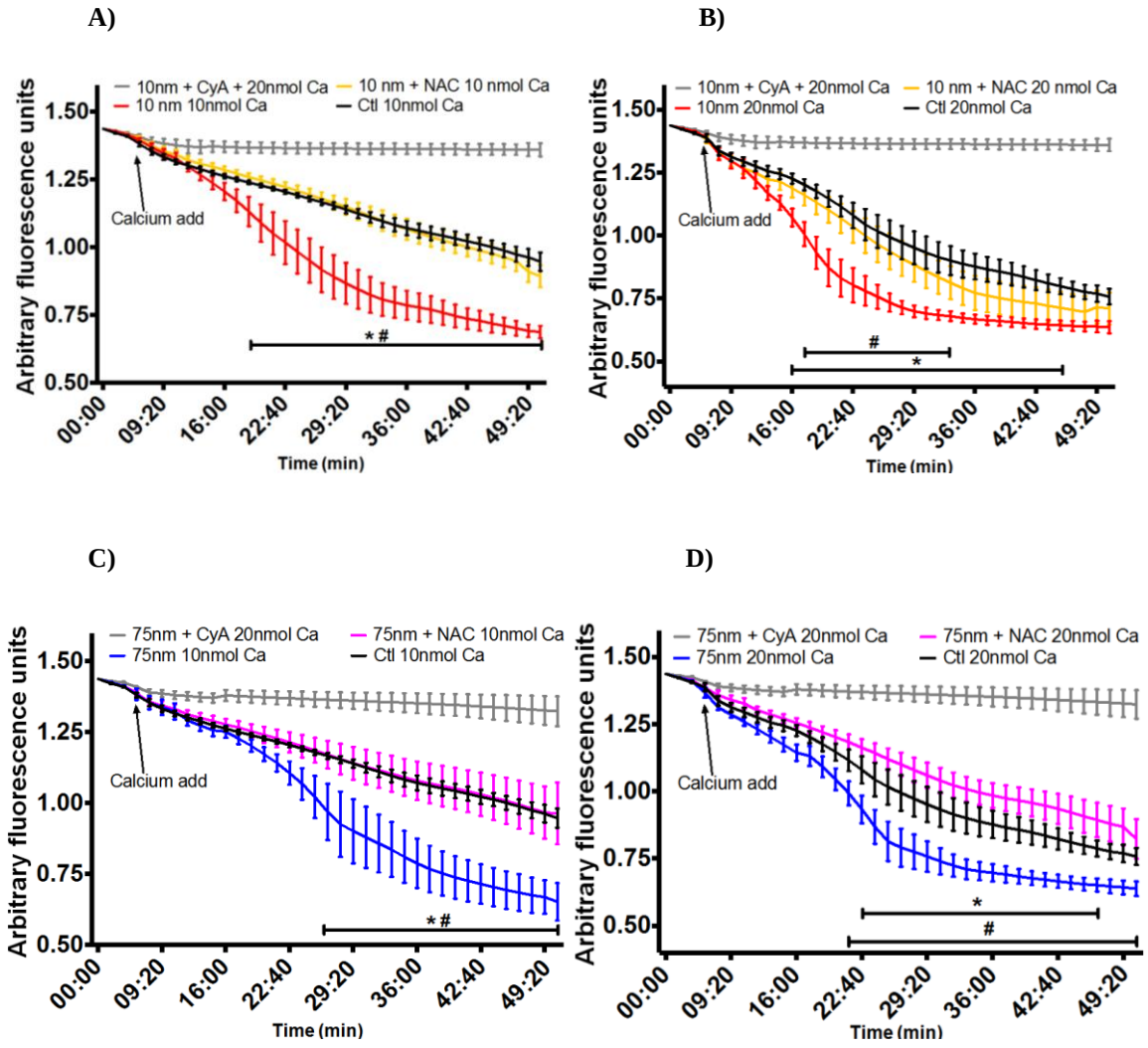

Figure 3.8- The effects of silver nanoparticles on the susceptibility to the induction of mitochondrial permeability transition (MPT). Mitochondrial swelling was spectrophotometrically monitored at 540 nm. Experiments were started by the addition of mitochondria (1 mg) to 2 ml of reaction medium supplemented with 3 μM rotenone and 5 mM succinate. After a small period of time to obtain a basal absorbance reading, 10 (A, C) and 20nmol (B, D) of calcium were added to individual preparations. The traces are representative of experiments performed with six independent mitochondrial preparations(p<0.05). *indicates statistically significant difference between silver nanoparticles and control; # indicates statistically significant difference between silver nanoparticles with and without NAC.

Mitochondria isolated from animals injected with either with 10 nm- or 75 nm-AgNPs were significantly more susceptible to calcium-dependent mitochondrial swelling, relative to the control (Fig. 3.8). NAC supplementation was significantly able to recover the calcium retention capacity in both sizes and doses of calcium. Pre-incubation with cyclosporine A (CyA), a MPT specific inhibitor, completely prevented

calcium-dependent mitochondrial swelling, indicating that the decrease in absorbance was the result of calcium-induced MPT.

3.10 Protein Content

Since AgNPs affected COX activity, COX-I and COX-IV content were evaluated (Figure 3.9). Both proteins are subunits of Cytochrome *c* oxidase, being COX-I encoded by mitochondrial DNA whereas COX-IV is one of the nuclear-coded polypeptide chains. Mitochondria exposed to either size of AgNPs revealed statistically non-significant trend towards increased COX-I and -IV content (Figure. 3.10). However, when pretreated with NAC, 75nm-AgNPs show a significant decrease in COX-IV content.

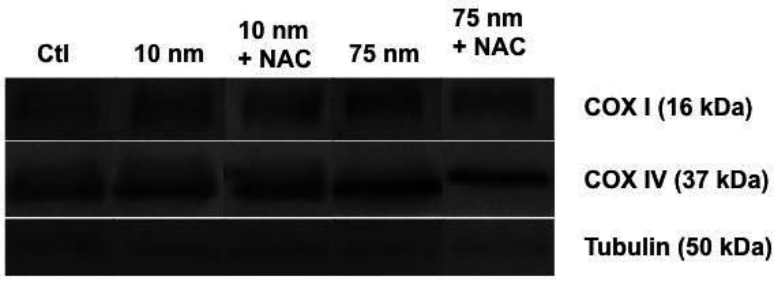

Figure 3.9- COX-I, COX-IV and tubulin content in liver homogenates were evaluated by western blotting. A representative blot from four independent experiments is shown.

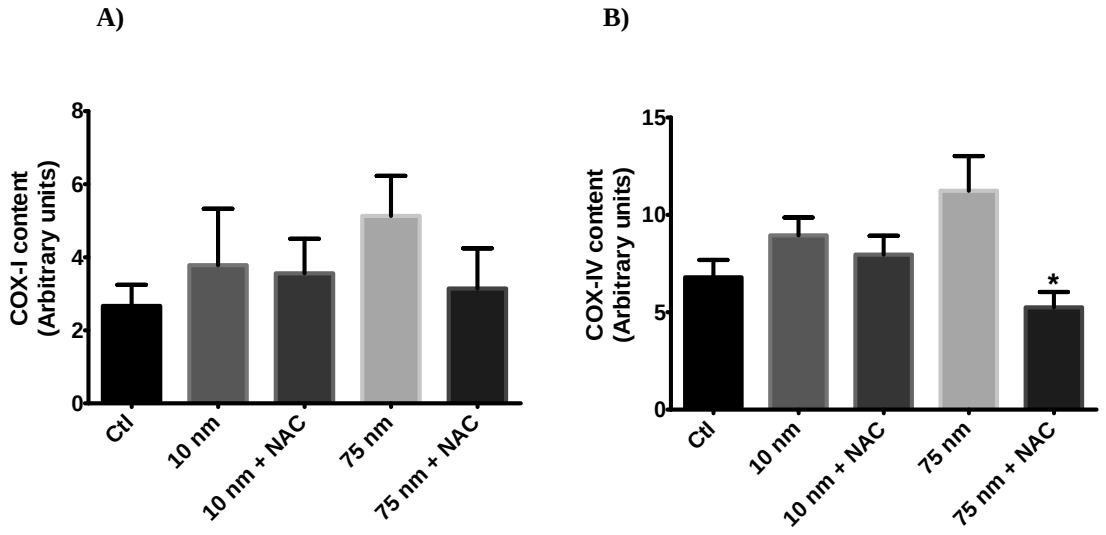

Figure 3.10- Densitometric analysis of COX-I (A) and COX-IV content (B). Data are means ± S.E.M of experiments performed with four animals/group(p<0.05). *indicates statistically significant difference versus 75 nm.

Chapter IV

Discussion and Conclusion

Nanomaterials have been of extreme importance to the industry due to the beneficial physicochemical features they have compared to bulk parental materials. Enhanced surface area, tunable size, modifiable surface chemistry and particle reactivity are some of the most important physicochemical properties that nanomaterials possess. These features give them improved thermal and/or electrical conductivity, improved catalytic activity and advanced optical properties (N. Singh et al., 2009). The development of nanotechnology is creating a broad array of nanoparticles that are already incorporated into a wide variety of consumer products. In 2011, more than 300 products containing nanosilver were available on the market (Gaiser et al., 2013) and as this number increases, the inevitable human exposure tends to rapidly expand, accompanied by potential for adverse health effects. Thus, there is a large international effort underway to verify nanoparticle safety upon the environment and human health. However, limited information is available about this concern thus far.

Silver is known for its antibacterial properties, giving AgNPs wide use in antimicrobial coatings, wound dressings, surgical instruments and more recently in biomedical devices that continuously release a low level of silver ions protecting against bacteria. Over the last years, nanoparticles have been the subject of intense research for use in biomedicine, namely as biosensors, drug-delivery agents and imaging contrast agents, which take advantage of their unique optical properties. Thus, due to the increasing use of AgNPs, biomedicine might be becoming the major source of human exposure to AgNPs. Besides injection, human exposure can occur via inhalation, ingestion and dermal contact (Ahamed et al., 2010; Lee et al., 2013).

For any exposure routes involving translocation to the bloodstream, the liver is one of the most important targets (Gaiser et al., 2013). Sadauskas et al. (2007) showed that Kupffer cells are essential for particle removal following intravenous administration. Recent studies on the biodistribution of AgNPs after injection demonstrated that the liver is the primary site of AgNPs deposition (Dziendzikowska et al., 2012; Lee et al., 2013). A study carried out by Sarhan & Hussein, (2014) showed a large number of lysosomes filled with AgNPs as well as complete loss of mitochondrial cristae in Kupffer cells. Therefore, the liver was chosen as a target organ in this study to identify adverse effects of AgNPs. As the liver is one of the main organs of nanoparticles deposition, certain adverse effects can occur due to AgNPs accumulation such as pathological changes in liver morphology, generation of ROS, DNA damage and changes in liver enzyme activities (Tiwari et al., 2011). The level of particular enzymes

in blood serum is a good indicator of liver injury (Tiwari et al., 2011) and our data shows that AgNPs were capable of increasing plasmatic AST and LDH activities. The AgNPs exposure could induce changes of cell shape, reduce cell viability and increases LDH release (Zhang et al., 2014). The LDH release is related with cell membrane damage, which along with increased plasmatic AST activity, a good biomarker of hepatocellular level damages, suggests hepatocellular injury induced by AgNPs exposure (Figure 3.2).

As a heavy metal, silver displays a strong affinity for thiol (-SH) groups present in biomolecules found throughout the body like reduced GSH and proteins, such as thioredoxin, SOD and thioredoxin peroxidase (T. Zhang et al., 2014). Therefore, AgNPs might cause an imbalance on human health due to an increase of oxidative stress. Miyayama and colleagues have shown that $AgNO_3$ increased the generation of ROS in mitochondria and altered the levels of antioxidant agents (Miyayama et al., 2013). There are also many other molecules that contain thiols in the cytoplasm, cell membrane and inner mitochondrial membrane. Silver can also interact with inner mitochondrial membrane proteins causing changes in membrane permeability and disruption of mitochondrial functions.

Since the major reason for AgNPs toxicity is the increase of oxidative stress, antioxidant therapy might be a viable strategy for attenuating this toxicity. It has been reported that the effects of Ag^+ on mitochondria can be blocked by the addition of antioxidant scavengers like GSH (Almofti et al., 2003). GSH plays a major role in cellular protection against oxidative stress due to its ability to bind and neutralize ROS (Hsin et al., 2008). Being a precursor of GSH's synthesis (Chairuangkitti et al., 2013), NAC was used in our study to understand whether oxidative stress caused by AgNPs can be prevented by an antioxidant. Some studies found that the pretreatment with NAC prevented AgNPs toxicity in human liver cells (Jing et al., 2011; Kim et al., 2009).

As previously mentioned, size is one of the main features that provide NPs unique properties. As the size decreases, there is an increase on the surface area/volume ratio, which enhances the catalytic activity of NPs leading to a higher reactivity upon other molecules (N. Singh et al., 2009). This larger surface area has also been related with enhancing release of toxic silver ions from the particle surface (Foldbjerg & Autrup, 2013). Furthermore, smaller AgNPs can cross biological barriers more efficiently than the larger ones allowing heightened interaction with biomolecules and critical organelles such as mitochondria. In accordance with these evidences, several studies

reported that smaller AgNPs induce more cytotoxicity than larger AgNPs (Ahamed et al., 2008; Carlson et al., 2008; Monteiller et al., 2007). To assess the influence of particle size upon the *in vivo* effect of AgNPs, two different sizes (10- and 75-nm) were used in our studies. Overall, 10nm-AgNPs show more cytotoxicity throughout the study than 75 nm-AgNPs. This effect will be discussed in more details below.

Being mitochondria the most important organelle in the cell in terms of energy metabolism, the next logical step was to understand how AgNPs administration would affect hepatic mitochondria. Previous studies have reported decreased mitochondrial $\Delta\psi$ using *in vitro* (Sahu et al., 2014) or *ex vivo* (Teodoro et al., 2011) models. As expected, AgNPs severely affect mitochondrial bioenergetics and function in our study. The results demonstrate that in isolated rat liver mitochondria, both sizes (10- and 75-nm) of AgNPs decreased mitochondrial initial potential, depolarization potential as well as repolarization potential (Table III). Two mechanisms are possible to explain this $\Delta\psi$ decrease: (i) proton (H^+) leak, increase of inner mitochondrial membrane permeability to H^+ and (ii) H^+ slip, decrease number of H^+ ejected coupled with deficient electron transport through the respiratory chain (Brookes, 2005; Murphy, 1989). The analysis of lag phase time, this is the time necessary for ADP phosphorylation, revealed significant increases in animals' mitochondria exposed with both sizes of AgNPs (Figure. 3.3).

Moreover, both sizes caused a severe decrease in state 3. The state 3 is established when a small amount of ADP is added to a mitochondrial preparation, allowing the function of ATP synthase. The H^+ re-entry causes a proton motive force decrease and electron transport acceleration leading to oxygen consumption increase. Thus, these results suggest that both sizes of AgNPs impaired the oxidative phosphorylation capacity of hepatic mitochondria as also shown by the decreased respiratory control ratio (RCR) (Table IV). The RCR is the single most useful general measure of function in isolated mitochondria. Generally speaking, high RCR indicates good function and implies that the mitochondria have a high capacity for substrate oxidation and ATP turnover and low proton leak. On the other hand, low RCR usually indicates dysfunction as changes in oxidative phosphorylation (Brand & Nicholls, 2011).

State 4 and vOligomycin respiration rates were also affected (Table IV). State 4 is achieved when all ADP added is converted to ATP leading to proton motive force increase, end of proton re-entry through ATP synthase and consequent mitochondrial respiration decreasing. On the other hand, oligomycin is a specific inhibitor of ATPase, blocking the proton re-entry through ATP synthase and decreasing mitochondrial

respiration, even in the presence of unphosphorylated ADP. In both conditions there is a respiration decrease due to proton gradient reestablishment caused by the activity of the respiratory chain. State 4 and vOligomycin respiration are controlled by the activity of the proton leak (Brand & Nicholls, 2011). As our data shows an increase in both respiratory rates, this suggests that AgNPs exposure did affect the inner mitochondrial membrane permeability to protons, consequently creating dissipation of membrane potential and heightened rate of respiration to regenerate $\Delta\psi$. This increase of inner mitochondrial membrane permeability can be related with the ability of silver ions to bind with transport proteins causing protonic leakage, resulting in the collapse of the proton motive force (Marambio-Jones & Hoek, 2010). The increase state 4 and vOligomycin respiration due to H^+ leak suggests this phenomenon as the main responsible for mitochondrial $\Delta\psi$ decrease. As previously mentioned AgNPs exposure increases ROS production (Arora et al., 2008; Carlson et al., 2008; Tiwari et al., 2011) It has been reported a close relationship between ROS generation and H^+ leak. ROS can induce lipidic oxidation in inner mitochondrial membrane which in turn can lead to H^+ leak (Brookes, 2005). Therefore, ROS generation due to AgNPs exposure can be the main responsible for the inner mitochondrial membrane permeability increasing. Mitochondria exposed to AgNPs show a significant recovering in mitochondrial $\Delta\psi$, state 4 and vOligomycin respiration when pretreated with NAC. This result suggests that NAC was able to prevent ROS generation induced by AgNPs exposure, avoiding lipidic oxidation and mitochondrial permeability. The results are in agreement with that reported previously by Hiura et al., (2000) showing that NAC blocked the mitochondrial membrane potential decrease.

ADP/O, an indicator of OXPHOS efficiency, was also significantly decreased (Table IV). ADP/O ratio represents the coupling between the use of oxygen by the electron transport chain and the ADP phosphorylated by ATP synthase. Changes in ADP/O values are related with alteration in the coupling mechanism, for instance, the respiratory complexes slip and pump fewer protons than normal (Brand & Nicholls, 2011). Therefore, ADP/O ratio decrease along with increasing lag phase suggests an uncoupling between the oxidative capacity by the electron transport chain and the phosphorylation of ADP to ATP by the ATP synthase. So it was reasonable to assume that somewhere along the respiratory chain, AgNPs were causing an impairment of the electronic flux through the respiratory chain. This was confirmed by the fact that AgNPs caused a severe decrease in vFCCP respiration in all experimental groups when

compared to control (Table IV). The decrease of vFCCP respiration associated with the depressed state 3 suggests possible alterations in the mitochondrial electron transport chain complexes' function. This hypothesis is supported by Almofti et al., (2003), who reported that Ag^{+} might affect mitochondria through interaction with -SH groups of inner mitochondrial membrane proteins, leading to impairments in ETC. A recent study found that all four mitochondrial electron transport chain complexes were significantly affected by exposure to Ag^{+} (Miyayama et al., 2013).

Once again, in our study, NAC administration was effective in the prevention of the AgNPs effects. When pretreated with NAC, mitochondria exposed with AgNPs show a significant recovering in ADP/O ratio, vFCCP and state 3 respiration. Thus, this result suggests that NAC prevent the effects of AgNPs upon the mitochondrial electron transport chain complexes. It is well established that AgNPs exposure increase the ROS generation and it is also known that oxidative phosphorylation enzymes are one of the elements particularly vulnerable to free radicals (Pieczenik & Neustadt, 2007). Therefore, as a precursor of GSH's synthesis, NAC regenerates the GSH levels, which in turn, can neutralize the effects of ROS upon mitochondrial complexes.

The hypothesis of damage in proteins of the respiratory chain was confirmed since the AgNPs of both sizes decreased the activity of succinate dehydrogenase (SDH) (Complex II). However, only 75-nm AgNPs caused a significantly decreased cytochrome *c* oxidase (COX) (Complex IV) activity (Figure 3.6). These results suggest that, unlike 75 nm-AgNPs, 10 nm-AgNPs do not cause damage to COX. However, SDH is apparently a target for both sizes.

When the protein content was investigated in mitochondria exposed with either sizes of AgNPs, a statistically non-significant trend towards increased mitochondrial-encoded COX subunit I and nuclear-encoded COX subunit IV was revealed (Figure 3.10). Thus, in light of the results, one possible explanation for this protein content increasing can be that mitochondria developed a compensatory response to overcome the decreased activity shown by COX. This way the content of COX subunits increases to help the functioning of mitochondrial oxidative system. This mechanism of the compensatory response has been already reported by Garcı & Gianotti, (2007). A study carried out by Teodoro et al, (2008) demonstrated a similar compensatory response, when excessive fat accumulation in hepatocytes leads to mitochondrial bioenergetics impairment. In the presence of NAC, COX-IV content shows a significant decrease when exposed to 75nm-AgNPs. In this condition, COX activity showed a similar value

to the control and, therefore, the compensatory response was not needed and the protein content did not increase.

To further explore and understand the cause for the enlarged lag phase, showing impairment in phosphorylative system, and a decrease in respiratory state 3, we evaluated ATPase activity since this results suggested that AgNPs exposure could affect ATPase efficiency. ATPase activity was dramatically decreased in mitochondria exposed to both sizes of AgNPs (Fig.3.4). The activity of the mitochondrial ATPase revealed that liver mitochondrial bioenergetics, in addition to damage to the oxidative system, also have imparments in the phosphorylative system. Thus, mitochondrial ATPsynthase is probably one target of toxicity induced by AgNPs. Despite these alterations on ATPase activity and unlike the studies reporting ATP depletion (Asharani et al., 2009; Hiura et al., 2000), ATP content did not reveal any alterations (Fig 3.5). These results suggest that despite the decrease of ATPase activity, mitochondria are still able to produce the ATP required for the cell. However, ATP production requires more time than in mitochondria that were not exposed to nanoparticles. Thus, despite the hepatocellular damages caused by AgNPs shown by the increase in plasmatic AST and LDH activities, the oxidative phosphorylation capacity of hepatic mitochondria is able to keep the ATP levels when chronically exposed to these low doses of AgNPs.

ROS generation is a hallmark of mitochondrial dysfunction caused by AgNPs exposure. As previously demonstrated, AgNPs induced generation of ROS, depletion of antioxidant GSH and reduction of mitochondrial function (Arora et al., 2008; Carlson et al., 2008; Hussain et al., 2005). Thus, it is believed that cellular oxidative stress may be the main responsible for cytotoxicity of AgNPs (Asharani, Low, et al., 2009; Jing et al., 2011; Monteiller et al., 2007). Hsin et al., (2008) showed inhibition of ROS production induced by AgNPs in cell pretreated with cyanide, an inhibitor of the mitochondrial electron-transferring activity of COX. This suggests that mitochondria are involved in AgNPs-mediated ROS generation. Our data shows a significant increase on ROS generation in mitochondria isolated from animals treated with both AgNPs sizes (Figure 3.7), suggesting that ROS generation is clearly an effect of AgNPs administration. Unlike that was expected, mitochondria isolated from the livers exposed to NAC revealed statistically non-significant trend towards decreased ROS production in both sizes of AgNPs. One possible explanation can be the fact that as ROS generation is maximal in this assay, NAC was inefficient to deal with such high values. However, in

physiological conditions, ROS generation induced by AgNPs is lower allowing the protective effect of NAC as have been seen throughout the results.

The calcium retention capacity of isolated mitochondria is a well established indicator of function and integrity, since it is linked to the permanent opening of the mitochondrial permeability transition (MPT) pore. Therefore, increase in mitochondrial permeability is a manifestation of mitochondrial dysfunction and is associated with induction of apoptosis and necrosis death (Kroemer et al., 2007; Varela et al., 2008). MPT induction disrupts the impermeability barrier of the inner membrane leading to membrane potential and pH gradient dissipation that together drive ATP synthesis through oxidative phosphorylation, causing impairment of mitochondrial function (Teodoro et al., 2011). This induced mitochondrial permeability is associated with pathological conditions and is triggered by high Ca^{2+} levels, oxidative stress, ATP depletion, high-inorganic phosphate and mitochondrial depolarization (Abou-Sleiman et al., 2006). A recent study demonstrated that mitochondria pre-incubated with different AgNPs sizes (40- and 80-nm) were more susceptible to mitochondrial swelling when compared to control (Teodoro et al., 2011). Our data shows a similar effect in mitochondria isolated from animals exposed to 10-nm or 75-nm AgNPs (Figure 3.8). The lower calcium buffering capacity of mitochondria exposed to AgNPs relative to the control suggest the compromising of mitochondrial integrity by AgNPs. These mitochondria are more susceptible to MPT induction, which allows the release of cytochrome *c* and other apoptogenic proteins stored within mitochondria, leading to the induction of the apoptotic dismantling of the cell (Rasola & Bernardi, 2011).

Oxidative stress and abnormally high levels of intramitochondrial Ca^{2+} are probably the two most important activators of MPT pore (Toman & Fiskum, 2011). These two factors interact synergistically, when mitochondria are oxidatively stressed, much lower levels of Ca^{2+} are required to activate MPT pore (Fiskum, 2000).

NAC supplementation was significantly able to recover the calcium retention capacity in both sizes and doses of calcium. Once again, these results suggest that NAC decreases the oxidative stress within the cell leading to a higher mitochondrial integrity.

As can be seen throughout the results, the efficiency of NAC to prevent the effect of AgNPs was higher in 75 nm- than 10 nm-AgNPs. ATP synthase and Succinate dehydrogenase activity and RCR are one of the examples where the preventive effect of NAC was only efficiently in mitochondria exposed to 75nm-AgNPs. Therefore, these results suggest that the smaller NPs, 10nm-AgNPs, showed a higher cytotoxicity than

larger NPs, 75nm-AgNPs. Our results are in agreement with previous reports that have shown higher cytotoxicity associated with smaller nanoparticles (Ahamed et al., 2008; Carlson et al., 2008; Monteiller et al., 2007).

In summary, this work aimed to evaluate the effects that are elicited by AgNPs exposure upon hepatic mitochondria. *In vivo* exposure to AgNPs caused impairment of rat liver mitochondrial function, due mainly to alterations of mitochondrial membrane permeability. The enhancement of H^+ leak results in an uncoupling effect on the oxidative phosphorylation system.

AgNPs also compromises the electron transfer along the electron transport chain by affecting complex II and IV of the respiratory chain. This impairment of mitochondrial electron transport chain activity causes accumulation of electrons in the electron transport chain complexes that can escape and directly react with oxygen to form the superoxide anion radical (Ribeiro et al., 2014). As oxidative stress is one of the mechanisms regulating the MPT pore opening, AgNPs also induced the MPT.

As previously mentioned, NAC was used in our study to understand whether the oxidative stress increase due to AgNPs exposure can be prevented by this antioxidant. Overall, we found that most of the effects caused by AgNPs exposure were prevented by pretreatment with NAC. This antioxidant agent efficiently prevented the structural damage to the inner mitochondrial membrane as evidenced by the recovery of mitochondrial membrane potential, and state 4 and vOligomycin respiration. Damage to mitochondrial electron transport chain complexes was also prevented by NAC as evidenced by the recovery of Complexes II and IV activities. Oxidative phosphorylation and calcium retention capacities of hepatic mitochondria were also improved by NAC treatment. Thus, NAC seems to be an efficient antioxidant against AgNPs toxicity. The prevention of these mitochondrial changes by NAC treatment suggests that ROS are involved in the mitochondrial toxicity caused by AgNPs treatment.

The main toxic effects of AgNPs and the protective mechanism of NAC are depicted in Figure 4.1.

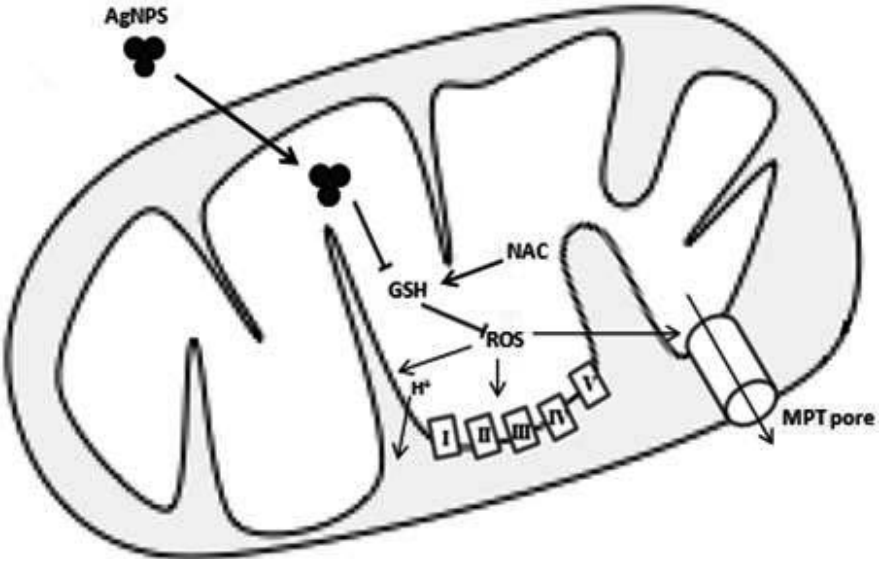

Figure 4.1- Scheme illustrating the main effects of AgNPs exposure and NAC administration. AgNPs can preferentially accumulate in mitochondria. Once within mitochondria, silver nanoparticles can interact with mitochondrial GSH, decreasing its levels. The decrease of GSH levels leads to mitochondrial oxidative stress increase. ROS generation causes impairment mitochondrial function, due mainly to alterations of mitochondrial membrane permeability leading to H^+ leak. AgNPs also compromises the electron transfer along the electron transport chain by affecting respiratory chain complexes. As oxidative stress is one of the mechanisms regulating the MPT pore opening, AgNPs also induce the MPT. NAC administration increases the levels of mitochondrial GSH, and the consequent decreasing of oxidative stress, preventing most of the effects caused by AgNPs exposure.

Chapter V

Bibliography

Abou-Sleiman, P. M., Muqit, M. M. K., & Wood, N. W. (2006). Expanding insights of mitochondrial dysfunction in Parkinson's disease. *Nature Reviews. Neuroscience*, *7*: 207–219.

Ahamed, M., Alsalhi, M. S., & Siddiqui, M. K. J. (2010). Silver nanoparticle applications and human health. *Clinica Chimica Acta; International Journal of Clinical Chemistry*, *411*: 1841–1848.

Ahamed, M., Karns, M., Goodson, M., Rowe, J., Hussain, S. M., Schlager, J. J., & Hong, Y. (2008). DNA damage response to different surface chemistry of silver nanoparticles in mammalian cells. *Toxicology and Applied Pharmacology*, *233*: 404–410.

Aillon, K. L., Xie, Y., El-Gendy, N., Berkland, C. J., & Forrest, M. L. (2009). Effects of nanomaterial physicochemical properties on in vivo toxicity. *Advanced Drug Delivery Reviews*, *61*: 457–466.

Almofti, M. R., Terada, H., & Shinohara, Y. (2003). Transition Ion Induces in Rat a Cyclosporine Liver Mitochondria and Release Permeability of Apoptogenic Cytochrome *c*. *J. Biochem. 134*, 43–49.

Arora, S., Jain, J., Rajwade, J. M., & Paknikar, K. M. (2008). Cellular responses induced by silver nanoparticles: In vitro studies. *Toxicology Letters*, *179*: 93–100.

Arora, S., Jain, J., Rajwade, J. M., & Paknikar, K. M. (2009). Interactions of silver nanoparticles with primary mouse fibroblasts and liver cells. *Toxicology and Applied Pharmacology*, *236*: 310–318.

Asharani, P. V, Hande, M. P., & Valiyaveettil, S. (2009). Anti-proliferative activity of silver nanoparticles. *BMC Cell Biology*, *10*: 65.

Asharani, P. V, Low, G., Mun, K., Hande, M. P., & Valiyaveettil, S. (2009). Cytotoxicity and Genotoxicity of Silver. *ACS Nano, 3*: 279–290.

Bartłomiejczyk, T., Lankoff, A., Kruszewski, M., & Szumiel, I. (2013). Silver nanoparticles -- allies or adversaries? *Annals of Agricultural and Environmental Medicine : AAEM*, *20*: 48–54.

Bernardi, P., Scorrano, L., Colonna, R., Petronilli, V., & Di Lisa, F. (1999). Mitochondria and cell death. Mechanistic aspects and methodological issues. *European Journal of Biochemistry / FEBS*, *264*: 687–701.

Brand, M. D., & Nicholls, D. G. (2011). Assessing mitochondrial dysfunction in cells. *The Biochemical Journal*, *435*: 297–312.

Brautigan, B. D. L., Ferguson-miller, S., & Margoliash, E. (1978). Mitochondrial Cytochrome c: Preparation and Activity of Native and Chemically Modified Cytochromes *c*. *Methods Enzymol, 53*: 128–164.

Brookes, P. S. (2005). Mitochondrial H^+ leak and ROS generation: an odd couple. *Free Radical Biology & Medicine, 38*: 12–23.

Carlson, C., Hussain, S. M., Schrand, a M., Braydich-Stolle, L. K., Hess, K. L., Jones, R. L., & Schlager, J. J. (2008). Unique cellular interaction of silver nanoparticles: size-dependent generation of reactive oxygen species. *The Journal of Physical Chemistry. B, 112*: 13608–13619.

Chairuangkitti, P., Lawanprasert, S., Roytrakul, S., Aueviriyavit, S., Phummiratch, D., Kulthong, K., … Maniratanachote, R. (2013). Silver nanoparticles induce toxicity in A549 cells via ROS-dependent and ROS-independent pathways. *Toxicology in Vitr , 27*: 330–338.

Chalmers, S., & Nicholls, D. G. (2003). The relationship between free and total calcium concentrations in the matrix of liver and brain mitochondria. *The Journal of Biological Chemistry, 278*: 19062–19670.

Chance, B., & Williams, G. R. (1956). The respiratory chain and oxidative. *Adv Enzymol*, 17: 65-134

Costa, C. S., Ronconi, J. V. V., Daufenbach, J. F., Gonçalves, C. L., Rezin, G. T., Streck, E. L., & Paula, M. M. D. S. (2010). In vitro effects of silver nanoparticles on the mitochondrial respiratory chain. *Molecular and Cellular Biochemistry*, *342*(1-2), 51–56.

Dziendzikowska, K., Gromadzka-Ostrowska, J., Lankoff, a, Oczkowski, M., Krawczyńska, a, Chwastowska, J., … Kruszewski, M. (2012). Time-dependent biodistribution and excretion of silver nanoparticles in male Wistar rats. *Journal of Applied Toxicology, 32*: 920–928.

El Badawy, A. M., Luxton, T. P., Silva, R. G., Scheckel, K. G., Suidan, M. T., & Tolaymat, T. M. (2010). Impact of environmental conditions (pH, ionic strength, and electrolyte type) on the surface charge and aggregation of silver nanoparticles suspensions. *Environmental Science & Technology*, *44*(4), 1260–1266.

Elechiguerra, J. L., Burt, J. L., Morones, J. R., Camacho-Bragado, A., Gao, X., Lara, H. H., & Yacaman, M. J. (2005). Interaction of silver nanoparticles with HIV-1. *Journal of Nanobiotechnology, 3*: 6.

Fiskum G. (2000). Mitochondrial participation in ischemic and traumatic neural cell death. *J Neurotrauma,* 17: 843–855.

Foldbjerg, R., & Autrup, H. (2013). Mechanisms of Silver Nanoparticle Toxicity. *Arch Basic Appl Med*, 1: 5–15.

Foley, S., Crowley, C., Smaihi, M., Bonfils, C., Erlanger, B. F., Seta, P., & Larroque, C. (2002). Cellular localisation of a water-soluble fullerene derivative. *Biochemical and Biophysical Research Communications*, 294: 116–119.

Gaiser, B. K., Hirn, S., Kermanizadeh, A., Kanase, N., Fytianos, K., Wenk, A., … Stone, V. (2013). Effects of silver nanoparticles on the liver and hepatocytes in vitro. *Toxicological Sciences : An Official Journal of the Society of Toxicology*, 131: 537–547.

Ghosh, M., J, M., Sinha, S., Chakraborty, A., Mallick, S. K., Bandyopadhyay, M., & Mukherjee, A. (2012). In vitro and in vivo genotoxicity of silver nanoparticles. *Mutation Research*, *749*: 60–69.

Gornall, A. G., Bardawill, C. J., & David, M. M. (1949). Determination of serum proteins by means of the biuret reaction. *J Biol Chem*, 177: 751-766.

Greulich, C., Diendorf, J., Simon, T., Eggeler, G., Epple, M., & Köller, M. (2011). Uptake and intracellular distribution of silver nanoparticles in human mesenchymal stem cells. *Acta Biomaterialia*, *7*: 347–354.

Gunter, T. E., Buntinas, L., Sparagna, G., Eliseev, R., & Gunter, K. (2000). Mitochondrial calcium transport: mechanisms and functions. *Cell Calcium*, *28*: 285–296.

Hiura, T. S., Li, N., Kaplan, R., Horwitz, M., Seagrave, J.-C., & Nel, a. E. (2000). The Role of a Mitochondrial Pathway in the Induction of Apoptosis by Chemicals Extracted from Diesel Exhaust Particles. *The Journal of Immunology*, *165*: 2703–2711.

Hsin, Y.-H., Chen, C.-F., Huang, S., Shih, T.-S., Lai, P.-S., & Chueh, P. J. (2008). The apoptotic effect of nanosilver is mediated by a ROS- and JNK-dependent mechanism involving the mitochondrial pathway in NIH3T3 cells. *Toxicology Letters*, *179*(3), 130–139.

Hussain, S. M., Hess, K. L., Gearhart, J. M., Geiss, K. T., & Schlager, J. J. (2005). In vitro toxicity of nanoparticles in BRL 3A rat liver cells. *Toxicology in Vitro*, *19*: 975–983.

Jiang, J., Oberdörster, G., & Biswas, P. (2008). Characterization of size, surface charge, and agglomeration state of nanoparticle dispersions for toxicological studies. *Journal of Nanoparticle Research*, *11*: 77–89.

Jing, M., Ah, K., Kyung, I., Sun, H., Kim, S., Yun, J., … Won, J. (2011). Silver nanoparticles induce oxidative cell damage in human liver cells through inhibition of reduced glutathione and induction of mitochondria-involved apoptosis. *Toxicology Letters, 201*: 92–100.

Kamo, N., Muratsugu, M., Hongoh, R., & Kobatake, Y. (1979). Membrane potential of mitochondria measured with an electrode sensitive to tetraphenyl phosphonium and relationship between proton electrochemical potential and phosphorylation potential in steady state. *The Journal of Membrane Biology, 49*: 105–121.

Kim, S., Eun, J., Choi, J., Chung, K., Park, K., Yi, J., & Ryu, D. (2009). Toxicology in Vitro Oxidative stress-dependent toxicity of silver nanoparticles in human hepatoma cells. *Toxicology in Vitro, 23*: 1076–1084.

Kim, S., & Ryu, D.-Y. (2013). Silver nanoparticle-induced oxidative stress, genotoxicity and apoptosis in cultured cells and animal tissues. *Journal of Applied Toxicology,* 33: 78–89.

Kroemer, G., Galluzzi, L., & Brenner, C. (2007). Mitochondrial membrane permeabilization in cell death. *Physiological Reviews, 87*: 99–163.

Lagouge, M., & Larsson, N.-G. (2013). The role of mitochondrial DNA mutations and free radicals in disease and ageing. *Journal of Internal Medicine, 273*: 529–543.

Lee, T.-Y., Liu, M.-S., Huang, L.-J., Lue, S.-I., Lin, L.-C., Kwan, A.-L., & Yang, R.-C. (2013). Bioenergetic failure correlates with autophagy and apoptosis in rat liver following silver nanoparticle intraperitoneally administration. *Particle and Fibre Toxicology, 10*: 40.

Madeira, V. (1975). A rapid and ultrasensitive method to measure calcium movements across biological membranes. *Biochem Biophys Res Commun* 64: 870-876.

Marambio-Jones, C., & Hoek, E. M. V. (2010). A review of the antibacterial effects of silver nanomaterials and potential implications for human health and the environment. *Journal of Nanoparticle Research, 12*: 1531–1551.

Martindale, J. L., & Holbrook, N. J. (2002). Cellular response to oxidative stress: signaling for suicide and survival. *Journal of Cellular Physiology, 192*: 1–15.

McBride, H. M., Neuspiel, M., & Wasiak, S. (2006). Mitochondria: more than just a powerhouse. *Current Biology : CB, 16*: 551–560.

Michel, S., Wanet, A., De Pauw, A., Rommelaere, G., Arnould, T., & Renard, P. (2012). Crosstalk between mitochondrial (dys)function and mitochondrial abundance. *Journal of Cellular Physiology, 227*: 2297–2310.

Miyayama, T., Arai, Y., Suzuki, N., & Hirano, S. (2013). Mitochondrial electron transport is inhibited by disappearance of metallothionein in human bronchial epithelial cells following exposure to silver nitrate. *Toxicology*, *305*: 20–9.

Monteiller, C., Tran, L., MacNee, W., Faux, S., Jones, A., Miller, B., & Donaldson, K. (2007). The pro-inflammatory effects of low-toxicity low-solubility particles, nanoparticles and fine particles, on epithelial cells in vitro: the role of surface area. *Occupational and Environmental Medicine*, *64*: 609–615.

Murdock, R. C., Braydich-Stolle, L., Schrand, A. M., Schlager, J. J., & Hussain, S. M. (2008). Characterization of nanomaterial dispersion in solution prior to in vitro exposure using dynamic light scattering technique. *Toxicological Sciences, 101:* 239–53.

Murphy, M. P. (1989). Slip and leak in mitochondrial oxidative phosphorylation. *Biochimica et Biophysica Acta*, 977: 123–141.

Nicholls, D. G., & Fergunson, S. (2013). *Bioenergetics 4.* Fourth ed. Amsterdam: Academic Press.

Ow, Y.-L. P., Green, D. R., Hao, Z., & Mak, T. W. (2008). Cytochrome c: functions beyond respiration. *Nature Reviews. Molecular Cell Biology*, *9*: 532–542.

Palmeira, C. M., & Rolo, A. P. (2012). *Mitochondrial Bioenergetics*. (C. M. Palmeira & A. J. Moreno, Eds.) (Vol. 810, pp. 89–101). Totowa, NJ: Humana Press.

Palmeira, C. M., & Wallace, K. B. (1997). Benzoquinone inhibits the voltage-dependent induction of the Mitochondrial Permeability Transition caused by redox-cycling naphthoquinones. *Toxicol Appl Pharmacol,* 143: 338–347.

Park, K., & Lee, Y. (2013). The stability of citrate-capped silver nanoparticles in isotonic glucose solution for intravenous injection. *Journal of Toxicology and Environmental Health, 76*: 1236–45.

Perier, C., & Vila, M. (2012). Mitochondrial biology and Parkinson's disease. *Cold Spring Harbor Perspectives in Medicine*, *2*: a009332.

Pieczenik, S. R., & Neustadt, J. (2007). Mitochondrial dysfunction and molecular pathways of disease. *Experimental and Molecular Pathology*, *83*: 84–92.

Rasola, A., & Bernardi, P. (2011). Mitochondrial permeability transition in Ca^{2+}-dependent apoptosis and necrosis. *Cell Calcium*, *50*: 222–233.

Ribeiro, M. P. C., Santos, A. E., & Custódio, J. B. a. (2014). Mitochondria: The gateway for tamoxifen-induced liver injury. *Toxicology*, *323C*: 10–18.

Rigoulet, M., Yoboue, E. D., & Devin, A. (2011). Mitochondrial ROS generation and its regulation: mechanisms involved in H_2O_2 signaling. *Antioxidants & Redox Signaling*, *14*(3), 459–68.

Rolo, A. P., & Palmeira, C. M. (2006). Diabetes and mitochondrial function: role of hyperglycemia and oxidative stress. *Toxicology and Applied Pharmacology*, *212*: 167–178.

Rolo, A. P., Teodoro, J. S., Peralta, C., Rosello-Catafau, J., & Palmeira, C. M. (2009). Prevention of I/R injury in fatty livers by ischemic preconditioning is associated with increased mitochondrial tolerance: the key role of ATPsynthase and mitochondrial permeability transition. *Transplant International*, *22*: 1081–1090.

Sadauskas, E., Wallin, H., Stoltenberg, M., Vogel, U., Doering, P., Larsen, A., & Danscher, G. (2007). Kupffer cells are central in the removal of nanoparticles from the organism. *Particle and Fibre Toxicology*, *4*: 10.

Sahu, S. C., Zheng, J., Graham, L., Chen, L., Ihrie, J., Yourick, J. J., & Sprando, R. L. (2014). Comparative cytotoxicity of nanosilver in human liver HepG2 and colon Caco2 cells in culture. *Journal of Applied Toxicology*

Santos, R. X., Correia, S. C., Zhu, X., Smith, M. a, Moreira, P. I., Castellani, R. J., … Perry, G. (2013). Mitochondrial DNA oxidative damage and repair in aging and Alzheimer's disease. *Antioxidants & Redox Signaling*, 18: 2444–2457.

Sarhan, O. M. M., & Hussein, R. M. (2014). Effects of intraperitoneally injected silver nanoparticles on histological structures and blood parameters in the albino rat. *International Journal of Nanomedicine*, *9*: 1505–1517.

Shoubridge, E. a. (2001). Nuclear genetic defects of oxidative phosphorylation. *Human Molecular Genetics*, *10*: 2277–2284.

Singer, P. (1974). Determination of the Activity of Succinate, NADH, Choline and α-Glycerophosphate Dehydrogenases. *Methods of Biochemical Analysis,* 22: 123–175.

Singh, N., Manshian, B., Jenkins, G. J. S., Griffiths, S. M., Williams, P. M., Maffeis, T. G. G., … Doak, S. H. (2009). NanoGenotoxicology: the DNA damaging potential of engineered nanomaterials. *Biomaterials*, *30*: 3891–3914.

Singh, R. P., & Ramarao, P. (2012). Cellular uptake, intracellular trafficking and cytotoxicity of silver nanoparticles. *Toxicology Letters*, *213*(2), 249–59.

Soane, L., Kahraman, S., Kristian, T., & Fiskum, G. (2007). Mechanisms of Impaired Mitochondrial Energy Metabolism in Acute and Chronic Neurodegenerative Disorders. *Journal of Neuroscience Research*, 85: 3407–3415.

Teodoro, J. S., Rolo, A. P., Duarte, F. V, Simões, A. M., & Palmeira, C. M. (2008). Differential alterations in mitochondrial function induced by a choline-deficient diet: understanding fatty liver disease progression. *Mitochondrion*, 8: 367–376.

Teodoro, J. S., Simões, A. M., Duarte, F. V, Rolo, A. P., Murdoch, R. C., Hussain, S. M., & Palmeira, C. M. (2011). Assessment of the toxicity of silver nanoparticles in vitro: a mitochondrial perspective. *Toxicology in Vitro*, 25: 664–670.

Territo, P. R., Mootha, V. K., French, S. A., Balaban, R. S., Paul, R., & Stephanie, A. (2000). Ca^{2+} activation of heart mitochondrial oxidative phosphorylation: role of the F_0/F_1-ATPase. *Am. J. Physiol. Cell Physiol*, 278: 423–435.

Tiwari, D. K., Jin, T., & Behari, J. (2011). Dose-dependent in-vivo toxicity assessment of silver nanoparticle in Wistar rats. *Toxicology Mechanisms and Methods*, *21*: 13–24.

Tolaymat, T. M., El Badawy, A. M., Genaidy, A., Scheckel, K. G., Luxton, T. P., & Suidan, M. (2010). An evidence-based environmental perspective of manufactured silver nanoparticle in syntheses and applications: a systematic review and critical appraisal of peer-reviewed scientific papers. *The Science of the Total Environment*, *408*: 999–1006.

Toman, J., & Fiskum, G. (2011). Influence of Aging on Membrane Permeability Transition in Brain Mitochondria. *J Bioenerg Biomembr*, *43*: 3–10.

Unfried, K., Albrecht, C., Klotz, L.-O., Von Mikecz, A., Grether-Beck, S., & Schins, R. P. F. (2007). Cellular responses to nanoparticles: Target structures and mechanisms. *Nanotoxicology*, 1: 52–71.

Varela, A. T., Gomes, A. P., Simões, A. M., Teodoro, J. S., Duarte, F. V, Rolo, A. P., & Palmeira, C. M. (2008). Indirubin-3'-oxime impairs mitochondrial oxidative phosphorylation and prevents mitochondrial permeability transition induction. *Toxicology and Applied Pharmacology*, *233*: 179–85.

Zhang, R., Piao, M. J., Kim, K. C., Kim, A. D., Choi, J.-Y., Choi, J., & Hyun, J. W. (2012). Endoplasmic reticulum stress signaling is involved in silver nanoparticles-induced apoptosis. *The International Journal of Biochemistry & Cell Biology*, *44*: 224–232.

Zhang, T., Wang, L., Chen, Q., & Chen, C. (2014). Cytotoxic potential of silver nanoparticles. *Yonsei Medical Journal*, *55*: 283–91.

Zheng, L.-Q., Yu, X.-D., Xu, J.-J., & Chen, H.-Y. (2014). Rapid visual detection of quaternary ammonium surfactants using citrate-capped silver nanoparticles (Ag NPs) based on hydrophobic effect. *Talanta*, 118: 90–5.

Zhou, S., Palmeira, C. M., & Wallace, K. B. (2001). Doxorubicin-induced persistent oxidative stress to cardiac myocytes. *Toxicology Letters*, *121*: 151–7.